

The Fundamental Subspaces of Ensemble Kalman Inversion

Elizabeth Qian*

Christopher Beattie†

September 16, 2024

Abstract

Ensemble Kalman Inversion (EKI) methods are a family of iterative methods for solving weighted least-squares problems, especially those arising in scientific and engineering inverse problems in which unknown parameters or states are estimated from observed data by minimizing the weighted square norm of the data misfit. Implementation of EKI requires only evaluation of the forward model mapping the unknown to the data, and does not require derivatives or adjoints of the forward model. The methods therefore offer an attractive alternative to gradient-based optimization approaches in large-scale inverse problems where evaluating derivatives or adjoints of the forward model is computationally intractable. This work presents a new analysis of the behavior of both deterministic and stochastic versions of basic EKI for linear observation operators, resulting in a natural interpretation of EKI’s convergence properties in terms of “fundamental subspaces” analogous to Strang’s fundamental subspaces of linear algebra. Our analysis directly examines the discrete EKI iterations instead of their continuous-time limits considered in previous analyses, and provides spectral decompositions that define six fundamental subspaces of EKI spanning both observation and state spaces. This approach verifies convergence rates previously derived for continuous-time limits, and yields new results describing both deterministic and stochastic EKI convergence behavior with respect to the standard minimum-norm weighted least squares solution in terms of the fundamental subspaces. Numerical experiments illustrate our theoretical results.

1 Introduction

Ensemble Kalman Inversion (EKI) methods describe a family of iterative methods for solving weighted least-squares problems of the form

$$\min_{\mathbf{v} \in \mathbb{R}^d} (\mathbf{y} - \mathbf{H}(\mathbf{v}))^\top \boldsymbol{\Sigma}^{-1} (\mathbf{y} - \mathbf{H}(\mathbf{v})) = \min_{\mathbf{v} \in \mathbb{R}^d} \|\mathbf{y} - \mathbf{H}(\mathbf{v})\|_{\boldsymbol{\Sigma}^{-1}}^2, \quad (1.1)$$

where $\boldsymbol{\Sigma} \in \mathbb{R}^{n \times n}$ is symmetric positive definite, and $\mathbf{H} : \mathbb{R}^d \rightarrow \mathbb{R}^n$. Such problems arise in many settings, including in *inverse problems* in which $\mathbf{v} \in \mathbb{R}^d$ represents an unknown parameter or state of a system of interest which must be inferred from observed data $\mathbf{y} \in \mathbb{R}^n$. Inverse problems arise in many disciplines across science, engineering, and medicine, including earth, atmospheric, and ocean modeling [42, 47, 48, 50, 66], medical imaging [22, 30, 57], robotics and autonomy [49], and more. In large-scale scientific and engineering applications, solving (1.1) using standard gradient-based optimization methods can be prohibitively expensive due to the high cost of evaluating derivatives or adjoints of the forward operator \mathbf{H} . In contrast, EKI methods can be implemented in an *adjoint-/derivative-free* way. This makes EKI an attractive alternative to gradient-based methods for solving (1.1) in large-scale applications. Historically, EKI methods have been developed in the contexts of reservoir simulation [20, 28, 29, 31, 33, 44] and weather and climate modeling [11, 23, 27, 32, 54, 60].

We focus on a basic version of EKI from [41] and presented in Algorithm 1, noting that other EKI methods can be viewed as variations on this theme. Throughout this work, \mathbb{E} and Cov denote the *true* expected

*School of Aerospace Engineering, School of Computational Science and Engineering, Georgia Institute of Technology, Atlanta, GA (eqian@gatech.edu, <https://www.elizabethqian.com>).

†Department of Mathematics, Virginia Polytechnic Institute and State University (beattie@vt.edu)

Algorithm 1 Basic Ensemble Kalman Inversion (EKI)

- 0: **Input:** forward operator $\mathbf{H} : \mathbb{R}^d \rightarrow \mathbb{R}^n$, initial ensemble $\{\mathbf{v}_0^{(1)}, \dots, \mathbf{v}_0^{(J)}\} \subset \mathbb{R}^d$, observations $\mathbf{y} \in \mathbb{R}^n$, observation error covariance $\Sigma \in \mathbb{R}^{n \times n}$
- 1: **for** $i = 0, 1, 2, \dots$, **do**
- 2: Compute observation-space ensemble: $\mathbf{h}_i^{(j)} = \mathbf{H}(\mathbf{v}_i^{(j)})$, $j = 1, 2, \dots, J$.
- 3: Compute empirical covariances: $\text{cov}[\mathbf{v}_i^{(1:J)}, \mathbf{h}_i^{(1:J)}]$ and $\text{cov}[\mathbf{h}_i^{(1:J)}]$
- 4: Compute Kalman gain: $\mathbf{K}_i = \text{cov}[\mathbf{v}_i^{(1:J)}, \mathbf{h}_i^{(1:J)}] \cdot (\text{cov}[\mathbf{h}_i^{(1:J)}] + \Sigma)^{-1}$
- 5: Sample $\boldsymbol{\varepsilon}_i^{(j)}$ i.i.d. from $\mathcal{N}(0, \Sigma)$ for $j = 1, 2, \dots, J$.
- 6: Perturb observations: set $\mathbf{y}_i^{(j)} = \mathbf{y} + \boldsymbol{\varepsilon}_i^{(j)}$ for $j = 1, 2, \dots, J$.
- 7: Compute particle update: $\mathbf{v}_{i+1}^{(j)} = \mathbf{v}_i^{(j)} + \mathbf{K}_i(\mathbf{y}_i^{(j)} - \mathbf{H}\mathbf{v}_i^{(j)})$ for $j = 1, 2, \dots, J$.
- 8: **if** converged **then**
- 9: **return** current ensemble mean, $\mathbb{E}[\mathbf{v}_{i+1}^{(1:J)}]$

*This is **Stochastic EKI**. For **Deterministic EKI**, skip 5-6 and assign $\mathbf{y}_i^{(j)} = \mathbf{y}$ in 7.*

value and covariance, respectively; whereas \mathbb{E} and cov denote the *empirical* (sample) mean and covariance operators, respectively: given $J \in \mathbb{N}$ samples $\{\mathbf{a}^{(j)}\}_{j=1}^J$ and $\{\mathbf{b}^{(j)}\}_{j=1}^J$, we define $\mathbb{E}[\mathbf{a}^{(1:J)}] = \frac{1}{J} \sum_{j=1}^J \mathbf{a}^{(j)}$, and

$$\text{cov}[\mathbf{a}^{(1:J)}, \mathbf{b}^{(1:J)}] = \frac{1}{J-1} \sum_{j=1}^J (\mathbf{a}^{(j)} - \mathbb{E}[\mathbf{a}^{(1:J)}])(\mathbf{b}^{(j)} - \mathbb{E}[\mathbf{b}^{(1:J)}])^\top,$$

and $\text{cov}[\mathbf{a}^{(1:J)}] = \text{cov}[\mathbf{a}^{(1:J)}, \mathbf{a}^{(1:J)}]$. Algorithm 1 prescribes the evolution of an ensemble of J particles, $\{\mathbf{v}_i^{(1)}, \dots, \mathbf{v}_i^{(J)}\}$, initialized at $i = 0$ in some way, e.g., by drawing from a suitable prior distribution, and subsequently updated for $i = 1, 2, 3$, etc. Those familiar with ensemble Kalman *filtering* methods will recognize familiar elements in Algorithm 1. Indeed, one way to obtain Algorithm 1 is to apply the ensemble Kalman filter to a system whose dynamics are given by the identity map in the “forecast” step of the filter. The connection to the ensemble Kalman filter also motivates the perturbation of the observations by random noise in Step 7; these perturbations ensure unbiased estimates of the filtering statistics in the linear Gaussian setting.

There is a very rich body of literature developing both theory and methodological variations for EKI. This includes convergence analyses of either mean-field limits of the iteration (equivalent to an infinitely large ensemble) [13, 26], or continuous-time limits, in which the deterministic iteration becomes a system of coupled ordinary differential equations (ODEs) [12, 58, 59] and the stochastic iteration becomes a system of coupled stochastic differential equations (SDEs) [8, 9, 10]. Several works have introduced variations on the basic algorithm, for example by incorporating a Tikhonov regularization term into the least-squares objective function [19, 69], enforcing constraints in the optimization [2, 14, 18, 36], or introducing hierarchical [16], multilevel [71], and parallel [72] versions of the algorithm. Beyond the successful use of EKI for solving diverse inverse problems in the physical sciences, e.g., in geophysical [4, 52, 65] and biological contexts [40], EKI has also been used as an optimizer for training machine learning models [34, 43, 46, 61, 62]. In particular, the use of EKI for training neural networks [43] has motivated the development of EKI variants based on ideas used for gradient-based training of neural networks, including dropout [45], data subsampling (also called ‘(mini-)batching’) [35, 43], adaptive step sizes [15], and convergence acceleration with Nesterov momentum [43]. As we will describe in more detail in the body of this work, the convergence of basic EKI is slow, occurring at a $1/\sqrt{i}$ rate [9, 58, 59], and convergence occurs only in the subspace spanned by the initial ensemble [41], which can be a limitation in settings where the ensemble size is small due to computational cost constraints. Several works have therefore proposed strategies which break the subspace property, including variance inflation or ‘localization’ strategies [3, 9, 15, 39, 64, 45], which may involve random perturbations of ensemble members [39, 45, 58], or adaptive ensemble sizes [51]. Variance inflation can also lead to faster convergence [15, 39]; in particular, perturbing EKI states with appropriately defined noise yields exponential convergence [39]. Beyond the weighted least squares problem (1.1), EKI has been adapted to new settings including Bayesian inverse problems [39], rare event sampling [67], and time-varying

forward models [70]. Ensemble Kalman methods more generally can also be viewed in terms of measure transport [5, 6, 24, 33, 44, 37, 53, 55, 56] with connections to sequential Monte Carlo methods [21, 25]: for further reading, see two excellent recent surveys [13, 17].

In the present work, we present new spectral and convergence analyses of both the deterministic and stochastic versions of basic EKI (Algorithm 1) for *linear* observation operators \mathbf{H} . Convergence results for some classes of nonlinear observers have been previously been derived in [68, 15, 67]; however, our focus on the linear case yields a natural interpretation of EKI’s convergence properties in terms of ‘fundamental subspaces of EKI’, akin to the four ‘fundamental subspaces’ that characterize Strang’s ‘Fundamental Theorem of Linear Algebra’ [63]. We directly analyze discrete EKI iterations rather than their continuous-time limits, and utilize spectral decompositions to define three fundamental subspaces in both the observation space \mathbb{R}^n , and the state space \mathbb{R}^d , yielding a total of *six* fundamental subspaces of EKI. We directly consider the discrete iteration for two principal reasons: (i) continuous-time limits can exhibit instabilities that are not observed for the discrete algorithms [3], and (ii) we can state and prove results about the discrete iteration without involving the properties of solutions to ODEs and SDEs, making the linear theory of EKI more broadly accessible to a wider audience, particularly in the stochastic setting. Our contributions are:

1. New spectral and convergence analysis of the *discrete* deterministic EKI iteration in both the observation and state spaces that (a) verify convergence rates previously derived in the continuous-time limit, (b) unify previous results to define fundamental subspaces of EKI for the general case where \mathbf{H} and the ensemble covariance may both be low-rank, and (c) yield new results relating EKI solutions to the standard minimum-norm least squares solution.
2. New spectral and convergence analysis of the *discrete* stochastic EKI iteration based on an idealized covariance iteration yielding (a) new results concerning the convergence of linear stochastic EKI particles in fundamental subspaces that are analogous to those of deterministic EKI, and (b) new insight into the failure of stochastic EKI to converge for small ensemble sizes.
3. Numerical experiments illustrating the analytical results.

The remainder of this work is organized as follows. Section 2 summarizes our main results. Sections 3 and 4 prove results for deterministic and stochastic linear EKI, respectively. Section 5 numerically illustrates our results and Section 6 concludes.

2 The fundamental subspaces of Ensemble Kalman Inversion

For the remainder of this work, we assume \mathbf{H} is a linear operator, $\mathbf{H} \in \mathbb{R}^{n \times d}$, with $\text{rank } h \leq \min(n, d)$. We begin by reviewing the standard four fundamental subspaces of the weighted least squares problem (Section 2.1). In Section 2.2, we then introduce the six fundamental subspaces of EKI at a high level and summarize our convergence results. Detailed technical definitions and proofs are deferred to Sections 3 and 4.

2.1 Fundamental subspaces of weighted least squares problems

In the context of the weighted least-squares problem (1.1), the four fundamental subspaces arise from dividing the two fundamental *spaces* (observation space \mathbb{R}^n and state space \mathbb{R}^d) into two *subspaces* each, one subspace associated with ‘observable’ directions and a complementary subspace associated with ‘unobservable’ directions as depicted in Figure 1. In observation space \mathbb{R}^n , the two fundamental subspaces are the range of \mathbf{H} , denoted $\text{Ran}(\mathbf{H})$, and its Σ^{-1} -orthogonal complement, $\text{Ker}(\mathbf{H}^\top \Sigma^{-1})$ (denoting the null space of $\mathbf{H}^\top \Sigma^{-1}$). In our least-squares problem, the closest that $\mathbf{H}\mathbf{v}$ can come to $\mathbf{y} \in \mathbb{R}^n$ with respect to the Σ^{-1} -norm is the Σ^{-1} -orthogonal projection of \mathbf{y} onto the observable space $\text{Ran}(\mathbf{H})$, which then has a zero component in the (unobservable) subspace $\text{Ker}(\mathbf{H}^\top \Sigma^{-1})$. In state space \mathbb{R}^d , the two fundamental subspaces are $\text{Ran}(\mathbf{H}^\top)$, and its orthogonal complement with respect to the Euclidean norm, $\text{Ker}(\mathbf{H})$. State space directions in $\text{Ker}(\mathbf{H})$ are unobservable because they are mapped by \mathbf{H} to zero and thus do not influence the minimand of (1.1). If $\text{Ker}(\mathbf{H})$ is non-trivial, multiple minimizers of (1.1) exist. A standard choice making the problem (1.1) well-posed is the norm-minimizing solution given by:

$$\mathbf{v}^* = (\mathbf{H}^\top \Sigma^{-1} \mathbf{H})^\dagger \mathbf{H}^\top \Sigma^{-1} \mathbf{y} \equiv \mathbf{H}^+ \mathbf{y}, \quad (2.1)$$

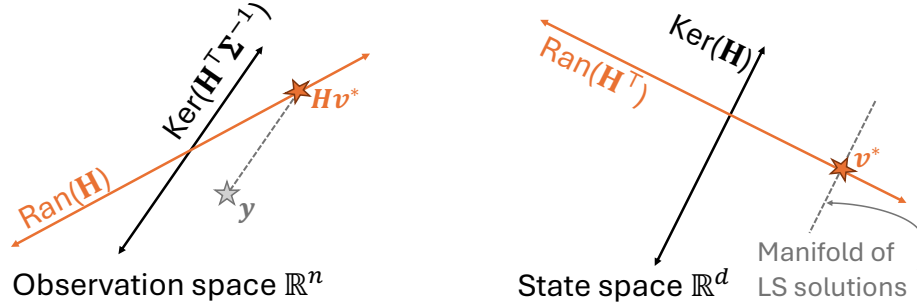


Figure 1: The four fundamental subspaces of the weighted least squares problem (1.1) for linear observers, $\mathbf{H} \in \mathbb{R}^{n \times d}$. In observation space (left), the image of the least squares solution lies in $\text{Ran}(\mathbf{H})$ and is Σ^{-1} -orthogonal to $\text{Ker}(\mathbf{H}^\top)$. In state space (right), the minimum-norm least squares solution (2.1) lies in $\text{Ran}(\mathbf{H}^\top)$ with zero component in $\text{Ker}(\mathbf{H})$.

where “ \dagger ” denotes the usual Moore-Penrose pseudoinverse and we have introduced the weighted pseudoinverse, $\mathbf{H}^+ = (\mathbf{H}^\top \Sigma^{-1} \mathbf{H})^\dagger \mathbf{H}^\top \Sigma^{-1}$. This unique norm-minimizing solution to (1.1) lies in the observable space $\text{Ran}(\mathbf{H}^\top)$ and has a zero component in the unobservable space $\text{Ker}(\mathbf{H})$.

2.2 Fundamental subspaces of Ensemble Kalman Inversion

Denote the empirical particle covariance by $\mathbf{\Gamma}_i = \text{cov}[\mathbf{v}_i^{(1:J)}]$. In ensemble Kalman inversion, fundamental subspaces arise first from dividing the state and observation spaces into directions that are ‘populated’ by particles, lying in the range of $\mathbf{\Gamma}_i$ (it is well-known that $\text{Ran}(\mathbf{\Gamma}_i)$ is invariant for all i [9, 12, 41, 58]), and ‘unpopulated’ directions lying in a complementary subspace. The populated subspace can then be further divided into two subspaces associated with observable and unobservable directions. There are therefore three subspaces in each of the observation and state spaces, and each of those sets of three subspaces are associated with three complementary oblique projection operators, $\mathcal{P}, \mathcal{Q}, \mathcal{N} \in \mathbb{R}^{n \times n}$ in observation space and $\mathbb{P}, \mathbb{Q}, \mathbb{N} \in \mathbb{R}^{d \times d}$ in state space, which we will define precisely in subsequent sections. In observation space \mathbb{R}^n , the three fundamental subspaces are then (i) $\text{Ran}(\mathcal{P}) \equiv \text{Ran}(\mathbf{H} \mathbf{\Gamma}_i)$, associated with observable populated directions, (ii) $\text{Ran}(\mathcal{Q}) \equiv \mathbf{H} \text{Ker}(\mathbf{\Gamma}_i \mathbf{H}^\top \Sigma^{-1} \mathbf{H})$, associated with observable but *unpopulated* directions, and (iii) $\text{Ran}(\mathcal{N}) \equiv \text{Ker}(\mathbf{H}^\top \Sigma^{-1})$, associated with unobservable directions. In state space \mathbb{R}^d , the three fundamental subspaces are (i) $\text{Ran}(\mathbb{P}) \subset \text{Ran}(\mathbf{\Gamma}_i)$, associated with observable populated directions (but generally *not* simply the intersection of $\text{Ran}(\mathbf{\Gamma}_i)$ with $\text{Ran}(\mathbf{H}^\top)$); (ii) $\text{Ran}(\mathbb{Q}) \subset \text{Ran}(\mathbf{H}^\top)$ associated with observable *unpopulated* directions, and (iii) $\text{Ran}(\mathbb{N})$ associated with unobservable directions. In subsequent sections, we will describe more precise relationships between these subspaces and the operators \mathbf{H} and $\mathbf{\Gamma}_i$. We will also show that EKI misfits [residuals] converge to zero at a $1/\sqrt{i}$ rate in the fundamental subspace associated with observable and populated directions, $\text{Ran}(\mathcal{P})$ [$\text{Ran}(\mathbb{P})$], and remain constant in the fundamental subspaces associated with observable unpopulated directions, $\text{Ran}(\mathcal{Q})$ [$\text{Ran}(\mathbb{Q})$], and likewise with unobservable directions, $\text{Ran}(\mathcal{N})$ [$\text{Ran}(\mathbb{N})$]. The fundamental subspaces of EKI are depicted in Figure 2, and an interactive three-dimensional visualization is available at <https://elizqian.github.io/eki-fundamental-subspaces/>.

3 Analysis of deterministic EKI

We first consider linear deterministic EKI (Algorithm 1 with $\mathbf{y}_i^{(j)} = \mathbf{y}$ and $\mathbf{H} \in \mathbb{R}^{n \times d}$ a linear observer). Sections 3.1 and 3.2 develop results in observation space \mathbb{R}^n and state space \mathbb{R}^d , respectively.

3.1 Deterministic EKI: Analysis in observation space \mathbb{R}^n

We begin by deriving an iteration map that governs the evolution of the data misfit (Section 3.1.1). Section 3.1.2 provides a spectral analysis of this iteration map that distinguishes three fundamental subspaces in

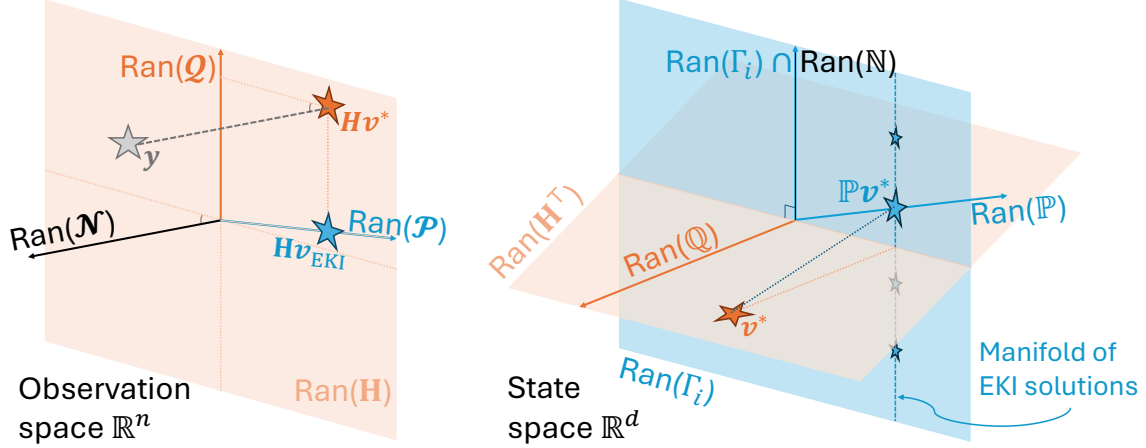


Figure 2: The six fundamental subspaces of Ensemble Kalman Inversion. In observation/state space (left/right), the three fundamental subspaces are (i) $\text{Ran}(\mathcal{P})/\text{Ran}(\mathbb{P})$, associated with observable populated directions, (ii) $\text{Ran}(\mathcal{Q})/\text{Ran}(\mathbb{Q})$ associated with observable unpopulated directions, and (iii) $\text{Ran}(\mathcal{N})/\text{Ran}(\mathbb{N})$ associated with unobservable directions.

observation space within which EKI has differing convergence behaviors, which are analyzed in Section 3.1.3.

3.1.1 Deterministic EKI: The data misfit iteration

Let $\theta_i^{(j)} = \mathbf{h}_i^{(j)} - \mathbf{y} = \mathbf{H}\mathbf{v}_i^{(j)} - \mathbf{y}$, for $j = 1, \dots, J$ and $i = 0, 1, \dots$ denote the *data misfits*, representing the deviation of the image of the particles under \mathbf{H} from the true data. Let $\Gamma_i = \text{cov}[\mathbf{v}_i^{(1:J)}]$ denote the empirical particle covariance. Note that for a linear observer, $\mathbf{H}, \text{cov}[\mathbf{v}_i^{(1:J)}, \mathbf{h}_i^{(1:J)}] \equiv \Gamma_i \mathbf{H}^\top$, $\text{cov}[\mathbf{h}_i^{(1:J)}] \equiv \mathbf{H} \Gamma_i \mathbf{H}^\top$, so that the Kalman gain is given as $\mathbf{K}_i \equiv \Gamma_i \mathbf{H}^\top (\mathbf{H} \Gamma_i \mathbf{H}^\top + \Sigma)^{-1}$. The update step of Algorithm 1 becomes:

$$\mathbf{v}_{i+1}^{(j)} = \mathbf{v}_i^{(j)} + \Gamma_i \mathbf{H}^\top (\mathbf{H} \Gamma_i \mathbf{H}^\top + \Sigma)^{-1} (\mathbf{y}^{(j)} - \mathbf{H}\mathbf{v}_i^{(j)}). \quad (3.1)$$

Then, setting $\mathbf{y}_i^{(j)} = \mathbf{y}$ for deterministic EKI yields

$$\begin{aligned} \theta_{i+1}^{(j)} &= \mathbf{H}\mathbf{v}_{i+1}^{(j)} - \mathbf{y} = \mathbf{H}\mathbf{v}_i^{(j)} + \mathbf{H}\Gamma_i \mathbf{H}^\top (\mathbf{H} \Gamma_i \mathbf{H}^\top + \Sigma)^{-1} (\mathbf{y} - \mathbf{H}\mathbf{v}_i^{(j)}) - \mathbf{y} \\ &= (\mathbf{I} - \mathbf{H}\Gamma_i \mathbf{H}^\top (\mathbf{H} \Gamma_i \mathbf{H}^\top + \Sigma)^{-1}) (\mathbf{H}\mathbf{v}_i^{(j)} - \mathbf{y}) \\ &= \Sigma (\mathbf{H}\Gamma_i \mathbf{H}^\top + \Sigma)^{-1} \theta_i^{(j)} \equiv \mathcal{M}_i \theta_i^{(j)}, \end{aligned} \quad (3.2)$$

where we have defined the data misfit iteration map, $\mathcal{M}_i = \Sigma (\mathbf{H}\Gamma_i \mathbf{H}^\top + \Sigma)^{-1}$. Describing the evolution of the data misfit, $\theta_i^{(j)}$, will require an analysis of \mathcal{M}_i .

3.1.2 Deterministic EKI: Decomposition of observation space \mathbb{R}^n

A spectral analysis of \mathcal{M}_i will distinguish three fundamental subspaces of the observation space \mathbb{R}^n that are invariant under \mathcal{M}_i . Consider the generalized eigenvalue problem defined by the pencil $(\mathbf{H}\Gamma_i \mathbf{H}^\top, \Sigma)$: that is, let $(\delta_{\ell,i}, \mathbf{w}_{\ell,i})$ satisfy

$$\mathbf{H}\Gamma_i \mathbf{H}^\top \mathbf{w}_{\ell,i} = \delta_{\ell,i} \Sigma \mathbf{w}_{\ell,i} \quad \text{for } \ell = 1, \dots, n \text{ and } i \geq 0. \quad (3.3)$$

Note that all eigenvalues of (3.3) are non-negative. While the eigenvalues, $\delta_{\ell,i}$, will evolve with i , we find that the corresponding eigenvectors remain constant:

Proposition 3.1. *The generalized eigenvectors of (3.3) are constant with respect to the iteration index, i , so that $\mathbf{w}_{\ell,i+1} = \mathbf{w}_{\ell,i} = \mathbf{w}_\ell$. The corresponding eigenvalues evolve with respect to i according to: $\delta_{\ell,i+1} = \delta_{\ell,i} / (1 + \delta_{\ell,i})^2$.*

Proof. Since $\boldsymbol{\theta}_i^{(j)} = \mathbf{h}_i^{(j)} - \mathbf{y}$, noting that covariances are unchanged by translation yields $\text{cov}[\boldsymbol{\theta}_i^{(j)}, \boldsymbol{\theta}_i^{(j)}] = \text{cov}[\mathbf{h}_i^{(j)}, \mathbf{h}_i^{(j)}] = \mathbf{H}\boldsymbol{\Gamma}_i\mathbf{H}^\top$. Then,

$$\begin{aligned}\mathbf{H}\boldsymbol{\Gamma}_{i+1}\mathbf{H}^\top &= \text{cov}[\boldsymbol{\theta}_{i+1}^{(j)}, \boldsymbol{\theta}_{i+1}^{(j)}] = \mathcal{M}_i \text{cov}[\boldsymbol{\theta}_i^{(j)}, \boldsymbol{\theta}_i^{(j)}] \mathcal{M}_i^\top = \mathcal{M}_i \mathbf{H}\boldsymbol{\Gamma}_i\mathbf{H}^\top \mathcal{M}_i^\top, \\ &= \boldsymbol{\Sigma}(\mathbf{H}\boldsymbol{\Gamma}_i\mathbf{H}^\top + \boldsymbol{\Sigma})^{-1} \mathbf{H}\boldsymbol{\Gamma}_i\mathbf{H}^\top (\mathbf{H}\boldsymbol{\Gamma}_i\mathbf{H}^\top + \boldsymbol{\Sigma})^{-1} \boldsymbol{\Sigma}.\end{aligned}$$

Suppose (δ_i, \mathbf{w}_i) is an eigenpair of (3.3) at iteration i , $\mathbf{H}\boldsymbol{\Gamma}_i\mathbf{H}^\top \mathbf{w}_i = \delta_i \boldsymbol{\Sigma} \mathbf{w}_i$. Then

$$(\mathbf{H}\boldsymbol{\Gamma}_i\mathbf{H}^\top + \boldsymbol{\Sigma})\mathbf{w}_i = (1 + \delta_i)\boldsymbol{\Sigma}\mathbf{w}_i \implies (\mathbf{H}\boldsymbol{\Gamma}_i\mathbf{H}^\top + \boldsymbol{\Sigma})^{-1}\boldsymbol{\Sigma}\mathbf{w}_i = \frac{1}{1 + \delta_i}\mathbf{w}_i \quad (*)$$

which implies

$$\mathbf{H}\boldsymbol{\Gamma}_i\mathbf{H}^\top (\mathbf{H}\boldsymbol{\Gamma}_i\mathbf{H}^\top + \boldsymbol{\Sigma})^{-1}\boldsymbol{\Sigma}\mathbf{w}_i = \mathbf{H}\boldsymbol{\Gamma}_i\mathbf{H}^\top \frac{1}{1 + \delta_i}\mathbf{w}_i = \frac{\delta_i}{1 + \delta_i}\boldsymbol{\Sigma}\mathbf{w}_i.$$

Left-multiplying by $\mathcal{M}_i = \boldsymbol{\Sigma}(\mathbf{H}\boldsymbol{\Gamma}_i\mathbf{H}^\top + \boldsymbol{\Sigma})^{-1}$ and applying $(*)$ yields

$$\mathbf{H}\boldsymbol{\Gamma}_{i+1}\mathbf{H}^\top \mathbf{w}_i = \frac{\delta_i}{(1 + \delta_i)^2}\boldsymbol{\Sigma}\mathbf{w}_i.$$

□

We now construct a basis of observation space \mathbb{R}^n made up of eigenvectors of (3.3).

Proposition 3.2. *Zero eigenvalues of (3.3) remain zero for all iterations, i.e., $\delta_{\ell,0} = 0$ implies $\delta_{\ell,i} = 0$ for all subsequent $i \geq 1$. Similarly, $\delta_{\ell,0} > 0$ implies $\delta_{\ell,i} > 0$ for all $i \geq 1$. Let r denote the number of positive eigenvalues of (3.3) and let $h = \text{rank}(\mathbf{H})$. Then, there is a $\boldsymbol{\Sigma}$ -orthogonal basis for \mathbb{R}^n made up of eigenvectors of (3.3), $\{\mathbf{w}_1, \dots, \mathbf{w}_n\}$, such that*

1. $\{\mathbf{w}_1, \dots, \mathbf{w}_r\} \subset \text{Ran}(\boldsymbol{\Sigma}^{-1}\mathbf{H})$ are eigenvectors of (3.3) associated with positive eigenvalues $\delta_{1,i}, \dots, \delta_{r,i}$, labeled in non-increasing order at $i = 1$, that is, $\delta_{1,1} \geq \delta_{2,1} \geq \dots \geq \delta_{r,1} > 0$. This ordering is preserved for subsequent $i \geq 1$.
2. if $r < h$, $\{\mathbf{w}_{r+1}, \dots, \mathbf{w}_h\} \subset \text{Ran}(\boldsymbol{\Sigma}^{-1}\mathbf{H})$ are eigenvectors of (3.3) associated with zero eigenvalues, and
3. if $h < n$, $\{\mathbf{w}_{h+1}, \dots, \mathbf{w}_n\} \subset \text{Ker}(\mathbf{H}^\top)$ are eigenvectors of (3.3) also associated with zero eigenvalues.

Additionally, $\text{span}(\mathbf{w}_1, \dots, \mathbf{w}_h) = \text{Ran}(\boldsymbol{\Sigma}^{-1}\mathbf{H})$ and $\text{span}(\mathbf{w}_{h+1}, \dots, \mathbf{w}_n) = \text{Ker}(\mathbf{H}^\top)$.

Proof. The preservation of eigenvalue (non-)zeroness can be read directly from the eigenvalue recurrence in Proposition 3.1. We now detail the construction of an eigenvector basis satisfying the above conditions. Take $\mathbf{w}_1, \dots, \mathbf{w}_r$ to be the linearly independent eigenvectors associated with the r positive eigenvalues of (3.3) ordered so that $\delta_{1,1} \geq \delta_{2,1} \geq \dots \geq \delta_{r,1} > 0$. Note that the recurrence relation in Proposition 3.1 implies that all nonzero eigenvalues must be in the interval $(0, 1)$ for all $i \geq 1$. Preservation of ordering follows from the fact that $\frac{x}{(1+x)^2}$ is monotone increasing for $x \in (0, 1)$. Note that $\{\mathbf{w}_1, \dots, \mathbf{w}_r\}$ are $\boldsymbol{\Sigma}$ -orthogonal and that $\text{span}(\mathbf{w}_1, \dots, \mathbf{w}_r) = \text{Ran}(\boldsymbol{\Sigma}^{-1}\mathbf{H}\boldsymbol{\Gamma}_i\mathbf{H}^\top) \subset \text{Ran}(\boldsymbol{\Sigma}^{-1}\mathbf{H})$.

If $r < h$, complete a $\boldsymbol{\Sigma}$ -orthogonal basis for $\text{Ran}(\boldsymbol{\Sigma}^{-1}\mathbf{H})$ with an additional $(h - r)$ linearly independent vectors $\{\mathbf{w}_{r+1}, \dots, \mathbf{w}_h\}$ so that $\text{span}(\mathbf{w}_1, \dots, \mathbf{w}_h) = \text{Ran}(\boldsymbol{\Sigma}^{-1}\mathbf{H})$. Suppose $\hat{\mathbf{w}} \in \text{span}(\mathbf{w}_{r+1}, \dots, \mathbf{w}_h)$ is chosen arbitrarily. Since $\{\mathbf{w}_1, \dots, \mathbf{w}_r\}$ form a basis for $\text{Ran}(\boldsymbol{\Sigma}^{-1}\mathbf{H}\boldsymbol{\Gamma}_i\mathbf{H}^\top)$, $\hat{\mathbf{w}}$ must be $\boldsymbol{\Sigma}$ -orthogonal to $\text{Ran}(\boldsymbol{\Sigma}^{-1}\mathbf{H}\boldsymbol{\Gamma}_i\mathbf{H}^\top)$. In particular, $\hat{\mathbf{w}}^\top \boldsymbol{\Sigma} \boldsymbol{\Sigma}^{-1} \mathbf{H}\boldsymbol{\Gamma}_i\mathbf{H}^\top = 0$ which implies $\mathbf{H}\boldsymbol{\Gamma}_i\mathbf{H}^\top \hat{\mathbf{w}} = 0$, so each of $\{\mathbf{w}_{r+1}, \dots, \mathbf{w}_h\}$ are eigenvectors of (3.3) associated with the zero eigenvalue.

Finally, if $h < n$, choose $(n - h)$ vectors, labeled as $\{\mathbf{w}_{h+1}, \dots, \mathbf{w}_n\}$, to be a $\boldsymbol{\Sigma}$ -orthogonal basis for $\text{Ker}(\mathbf{H}^\top)$. They then will be eigenvectors for (3.3) associated with the zero eigenvalue. The full set of vectors, $\{\mathbf{w}_1, \dots, \mathbf{w}_r, \mathbf{w}_{r+1}, \dots, \mathbf{w}_h, \mathbf{w}_{h+1}, \dots, \mathbf{w}_n\}$ will be a $\boldsymbol{\Sigma}$ -orthogonal basis of eigenvectors of (3.3) that span \mathbb{R}^n . □

This construction leads us to a compact summary representation of (3.3): define $\Delta_i = \text{diag}(\delta_{1,i}, \delta_{2,i}, \dots, \delta_{n,i})$ and $\mathbf{W} = [\mathbf{w}_1, \mathbf{w}_2, \dots, \mathbf{w}_n]$. Then (3.3) can be written as $\mathbf{H}\Gamma_i\mathbf{H}^\top\mathbf{W} = \Sigma\mathbf{W}\Delta_i$. \mathbf{W} is the matrix of eigenvectors of (3.3) and Σ -orthogonality of the eigenvectors establishes that $\mathbf{W}^\top\Sigma\mathbf{W}$ is diagonal. Without loss of generality we may renormalize eigenvectors so that $\mathbf{w}_\ell^\top\Sigma\mathbf{w}_\ell = 1$, or equivalently, $\mathbf{W}^\top\Sigma\mathbf{W} = \mathbf{I}$.

The three types of eigenvectors of (3.3) described in Proposition 3.2 are each associated with different invariant subspaces of the data misfit iteration map \mathcal{M}_i , which we now characterize in terms of spectral projectors of \mathcal{M}_i .

Proposition 3.3. *Let $\mathbf{W}_{k:\ell} \in \mathbb{R}^{n \times (\ell-k+1)}$ contain columns k through ℓ of \mathbf{W} . Define $\mathcal{P} = \Sigma\mathbf{W}_{1:r}\mathbf{W}_{1:r}^\top$, $\mathcal{Q} = \Sigma\mathbf{W}_{r+1:h}\mathbf{W}_{r+1:h}^\top$, and $\mathcal{N} = \Sigma\mathbf{W}_{h+1:n}\mathbf{W}_{h+1:n}^\top$. Then, \mathcal{P} , \mathcal{Q} , and \mathcal{N} are spectral projectors associated with the misfit iteration map \mathcal{M}_i , i.e., $\mathcal{M}_i\mathcal{P} = \mathcal{P}\mathcal{M}_i$ and $\mathcal{P}^2 = \mathcal{P}$, with similar assertions for \mathcal{Q} and \mathcal{N} . \mathcal{P} , \mathcal{Q} , and \mathcal{N} are complementary in the sense that $\mathcal{P}\mathcal{Q} = \mathcal{P}\mathcal{N} = \mathcal{Q}\mathcal{N} = \mathbf{0}$ and $\mathcal{P} + \mathcal{Q} + \mathcal{N} = \mathbf{I}_n$.*

Proof. Note $\mathcal{M}_i = \Sigma\mathbf{W}(\mathbf{I}_n + \Delta_i)^{-1}\mathbf{W}^\top$. Define $\Delta_{1:r}^{(i)} = \text{diag}(\delta_{1,i}, \dots, \delta_{r,i})$. Then,

$$\begin{aligned}\mathcal{M}_i\mathcal{P} &= \Sigma\mathbf{W}(\mathbf{I}_n + \Delta_i)^{-1}\mathbf{W}^\top\Sigma\mathbf{W}_{1:r}\mathbf{W}_{1:r}^\top = \Sigma\mathbf{W}_{1:r}(\mathbf{I}_r + \Delta_{1:r}^{(i)})^{-1}\mathbf{W}_{1:r}^\top \\ &= \Sigma\mathbf{W}_{1:r}\mathbf{W}_{1:r}^\top\Sigma\mathbf{W}(\mathbf{I}_n + \Delta_i)^{-1}\mathbf{W}^\top = \mathcal{P}\mathcal{M}_i.\end{aligned}$$

The normalization condition implies $\mathbf{W}_{1:r}^\top\Sigma\mathbf{W}_{1:r} = \mathbf{I}_r$, so we have upon substitution $\mathcal{P}^2 = \Sigma\mathbf{W}_{1:r}(\mathbf{W}_{1:r}^\top\Sigma\mathbf{W}_{1:r})\mathbf{W}_{1:r}^\top = \mathcal{P}$. Similar arguments can be followed to show that $\mathcal{M}_i\mathcal{Q} = \mathcal{Q}\mathcal{M}_i$ and $\mathcal{Q}^2 = \mathcal{Q}$, as well as $\mathcal{M}_i\mathcal{N} = \mathcal{N}\mathcal{M}_i$ and $\mathcal{N}^2 = \mathcal{N}$. The assertion $\mathcal{P}\mathcal{Q} = \mathcal{P}\mathcal{N} = \mathcal{Q}\mathcal{N} = \mathbf{0}$ follows immediately from the Σ -orthogonality of the eigenvector basis. Likewise, $\mathbf{W}^\top\Sigma\mathbf{W} = \mathbf{I}$ implies $\Sigma^{-1} = \mathbf{W}\mathbf{W}^\top = \mathbf{W}_{1:r}\mathbf{W}_{1:r}^\top + \mathbf{W}_{r+1:h}\mathbf{W}_{r+1:h}^\top + \mathbf{W}_{h+1:n}\mathbf{W}_{h+1:n}^\top$. Multiplication by Σ verifies $\mathcal{P} + \mathcal{Q} + \mathcal{N} = \mathbf{I}$. \square

The data misfits can thus be divided into three components associated with the oblique projectors defined in Proposition 3.3: $\theta_i^{(j)} = \mathcal{P}\theta_i^{(j)} + \mathcal{Q}\theta_i^{(j)} + \mathcal{N}\theta_i^{(j)}$. These components will *not* generally be orthogonal to one another, though they each occupy invariant subspaces that reflect differing convergence behaviors as we next show.

3.1.3 Deterministic EKI: Convergence analysis in observation space \mathbb{R}^n

We first prove a lemma concerning the reciprocal nonzero eigenvalues.

Lemma 3.4. *If $\delta_{\ell,0} \neq 0$, then for all $i \geq 1$, we have $\frac{1}{\delta_{\ell,i}} = \frac{1}{\delta_{\ell,0}} + 2i + \sum_{k=0}^{i-1} \delta_{\ell,k}$.*

Proof. We prove by induction, verifying first the base case with $i = 1$:

$$\frac{1}{\delta_{\ell,1}} = \frac{(1 + \delta_{\ell,0})^2}{\delta_{\ell,0}} = \frac{1 + 2\delta_{\ell,0} + \delta_{\ell,0}^2}{\delta_{\ell,0}} = \frac{1}{\delta_{\ell,0}} + 2 + \delta_{\ell,0}.$$

The same calculation for $i \geq 1$ yields $\frac{1}{\delta_{\ell,i+1}} = \frac{1}{\delta_{\ell,i}} + 2 + \delta_{\ell,i}$. Substituting the inductive hypothesis for $\frac{1}{\delta_{\ell,i}}$ and re-arranging completes the induction step and the proof. \square

We use this lemma to provide upper and lower bounds on the asymptotic behaviour of the nonzero eigenvalues. We make use of the following fact:

Fact 3.5. *For all $i \geq 1$, $\log i < \sum_{k=1}^i \frac{1}{k} < 2 + \log i$.*

Proposition 3.6. *If $\delta_{\ell,0} \neq 0$, then there exists a constant $c_\ell > 0$ so that for all $i \geq 1$ the following bounds hold:*

$$\frac{1}{2i} - \frac{c_\ell + \log i}{8i^2} < \delta_{\ell,i} < \frac{1}{2i}.$$

Proof. From Lemma 3.4 we have $\frac{1}{\delta_{\ell,i}} > 2i$ for $i \geq 1$ and therefore $\delta_{\ell,i} < \frac{1}{2i}$. Then, we can bound the sum $\sum_{k=0}^{i-1} \delta_{\ell,k} \leq \delta_{\ell,0} + \sum_{k=1}^{i-1} \frac{1}{2k}$ and apply Fact 3.5 to obtain

$$\sum_{k=0}^{i-1} \delta_{\ell,k} \leq \delta_{\ell,0} + 1 + \frac{1}{2} \log i. \quad (\#)$$

Using this bound in the recurrence from Lemma 3.4 yields

$$\frac{1}{\delta_{\ell,i}} < 2i + (\delta_{\ell,0}^{-1} + \delta_{\ell,0} + 1) + \frac{1}{2} \log i.$$

Let $c_\ell/2 = (\delta_{\ell,0}^{-1} + \delta_{\ell,0} + 1)$, so that c_ℓ is a constant independent of i . Then,

$$\delta_{\ell,i} > \frac{1}{2i + \frac{c_\ell + \log i}{2}} = \frac{1}{2i} \left(\frac{1}{1 + \frac{c_\ell + \log i}{4i}} \right) \geq \frac{1}{2i} \left(1 - \frac{c_\ell + \log i}{4i} \right) = \frac{1}{2i} - \frac{c_\ell + \log i}{8i^2}.$$

□

Corollary 3.7. *As $i \rightarrow \infty$, the nonzero eigenvalues of (3.3) satisfy $\delta_{\ell,i} \sim \frac{1}{2i}$.*

Proof. From Lemma 3.4,

$$\lim_{i \rightarrow \infty} \left(\frac{1}{2i} / \delta_{\ell,i} \right) = \lim_{i \rightarrow \infty} \frac{1}{2i\delta_{\ell,0}} + 1 + \lim_{i \rightarrow \infty} \frac{1}{2i} \sum_{k=0}^{i-1} \delta_{\ell,k}.$$

The first limit on the right hand side is evidently zero. Using (#), the third term on the right hand side can be bounded as $0 < \frac{1}{2i} \sum_{k=0}^{i-1} \delta_{\ell,k} < \frac{1}{2i} (\delta_{\ell,0} + 1 + \frac{1}{2} \log i) \rightarrow 0$, as $i \rightarrow \infty$. Thus, $\lim_{i \rightarrow \infty} \frac{1}{2i} / \delta_{\ell,i} = 1$. □

We can now prove our main result about the behavior of the EKI data misfit in the observation space \mathbb{R}^n .

Theorem 3.8. *For all particles $j = 1, 2, \dots, J$, the following hold:*

- (a) *as $i \rightarrow \infty$, $\|\mathcal{P}\theta_i^{(j)}\| = \mathcal{O}(i^{-\frac{1}{2}})$,*
- (b) *for all $i \geq 0$, $\mathcal{Q}\theta_i^{(j)} = \mathcal{Q}\theta_0^{(j)}$, and*
- (c) *for all $i \geq 0$, $\mathcal{N}\theta_i^{(j)} = \mathcal{N}\theta_0^{(j)}$.*

Proof. Note that $\mathcal{M}_i = \Sigma \mathbf{W}_{1:r} (\mathbf{I}_r + \Delta_{1:r}^{(i)})^{-1} \mathbf{W}_{1:r}^\top + \mathcal{Q} + \mathcal{N}$. Define $\mathcal{M}_{i0} = \mathcal{M}_i \cdots \mathcal{M}_2 \mathcal{M}_1 \mathcal{M}_0$ so that $\theta_i^{(j)} = \mathcal{M}_{i0} \theta_0^{(j)}$, and note that

$$\mathcal{M}_{i0} = \Sigma \mathbf{W}_{1:r} \mathbf{D}_{i0} \mathbf{W}_{1:r}^\top + \mathcal{Q} + \mathcal{N}, \quad \text{where} \quad \mathbf{D}_{i0} = \prod_{k=0}^i (\mathbf{I}_r + \Delta_{1:r}^{(k)})^{-1}.$$

Then, for all i , $\mathcal{Q}\mathcal{M}_{i0} = \mathcal{Q}$ and $\mathcal{N}\mathcal{M}_{i0} = \mathcal{N}$, and the last two statements of Theorem 3.8 follow. Additionally,

$$\mathcal{P}\theta_i^{(j)} = \mathcal{P}\mathcal{M}_{i0}\theta_0^{(j)} = \mathcal{M}_{i0}\mathcal{P}\theta_0^{(j)} = \Sigma \mathbf{W}_{1:r} \mathbf{D}_{i0} \mathbf{W}_{1:r}^\top \mathcal{P}\theta_0^{(j)}.$$

Denote the diagonal entries of \mathbf{D}_{i0} as $d_{\ell,i} = \prod_{k=0}^i (1 + \delta_{\ell,k})^{-1}$ for $1 \leq \ell \leq r$. Then,

$$\|\mathcal{P}\theta_i^{(j)}\| \leq d_{r,i} \|\Sigma \mathbf{W}_{1:r}\| \|\mathbf{W}_{1:r}\| \|\mathcal{P}\theta_0^{(j)}\|.$$

For each particle j , the quantity $\|\Sigma \mathbf{W}_{1:r}\| \|\mathbf{W}_{1:r}\| \|\mathcal{P}\theta_0^{(j)}\|$ is a constant independent of i , so we now need only show that $d_{r,i} = \mathcal{O}(i^{-\frac{1}{2}})$. Note from the definition that $-\log d_{r,i} = \sum_{k=0}^i \log(1 + \delta_{r,k})$. Since $\log(1+x) > x - \frac{1}{2}x^2$ for $x \in (0, 1)$, we have

$$-\log d_{r,i} > \log(1 + \delta_{r,0}) + \sum_{k=1}^i \left(\delta_{r,k} - \frac{1}{2} \delta_{r,k}^2 \right).$$

Moreover, since $x - \frac{1}{2}x^2$ is monotone increasing on $(0, 1)$, Proposition 3.6 implies

$$\begin{aligned} -\log d_{r,i} &> \log(1 + \delta_{r,0}) + \sum_{k=1}^i \left(\frac{1}{2k} - \frac{c_r + \log k}{8k^2} - \frac{1}{2} \left(\frac{1}{2k} - \frac{c_r + \log k}{8k^2} \right)^2 \right), \\ &> \log(1 + \delta_{r,0}) + \sum_{k=1}^i \frac{1}{2k} - \sum_{k=1}^{\infty} \left(\frac{c_r + \log k}{8k^2} + \frac{1}{2} \left(\frac{1}{2k} - \frac{c_r + \log k}{8k^2} \right)^2 \right) \end{aligned}$$

Note that all terms of the final summand converge at least as fast as $\frac{\log k}{k^2}$, so the final sum must converge to some finite constant c_{∞} . Define $C = \log(1 + \delta_{r,0}) - c_{\infty}$. Combining with the lower bound on the harmonic sum $\sum_{k=1}^i \frac{1}{2k}$ from Fact 3.5, yields

$$-\log d_{r,i} > C + \frac{1}{2} \log i \implies d_{r,i} < \frac{\exp(-C)}{\sqrt{i}} = \frac{\exp(c_{\infty})}{1 + \delta_{r,0}} \frac{1}{\sqrt{i}}.$$

□

Remark 3.9. *Previous analyses of linear deterministic EKI have divided the misfit into just two components, corresponding to our \mathcal{P} and its complementary projection under the assumption that \mathbf{H} is one-to-one [58, 59], or to our \mathcal{P} and \mathcal{N} under the assumption that $\mathbf{\Gamma}_i$ is full-rank [12]. Theorem 3.8 unifies these results in the general case where both \mathbf{H} and $\mathbf{\Gamma}_i$ may be rank-deficient, leading to the definition of three fundamental subspaces: $\text{Ran}(\mathcal{P})$, comprised of populated observable directions, in which the data misfit converges at a $1/\sqrt{i}$ rate; and two subspaces in which the data misfit remains constant: directions in $\text{Ran}(\mathcal{Q})$ are observable but unpopulated by the ensemble, while directions in $\text{Ran}(\mathcal{N})$ are simply unobservable.*

3.2 Deterministic EKI: Analysis in state space \mathbb{R}^d

We now consider the evolution of the state-space least squares residual of the particles with respect to the standard minimum-norm solution (2.1). Section 3.2.1 derives an iteration map for this residual, which motivates a spectral analysis in Section 3.2.2 that defines three fundamental subspaces of EKI in state space analogous to those defined in observation space. Section 3.2.3 provides a convergence analysis that describes the behavior of the EKI particles in the three fundamental subspaces.

3.2.1 Deterministic EKI: The least-squares residual iteration

We first show the well-known ‘subspace property’ of basic EKI [9, 12, 41, 58]: that is, across all iterations particles always remain in the subspace spanned by the initial ensemble.

Proposition 3.10. *For all $i \geq 0$, $\text{Ran}(\mathbf{\Gamma}_{i+1}) \subset \text{Ran}(\mathbf{\Gamma}_i)$. Additionally, define $\mathbf{V}_i = [\mathbf{v}_i^{(1)}, \mathbf{v}_i^{(2)}, \dots, \mathbf{v}_i^{(J)}] \in \mathbb{R}^{d \times J}$. Then $\text{Ran}(\mathbf{V}_{i+1}) \subset \text{Ran}(\mathbf{V}_i) \subset \text{Ran}(\mathbf{V}_0)$.*

Proof. Define $\mathbf{e} = [1, 1, \dots, 1]^\top \in \mathbb{R}^d$ and $\mathbf{\Pi} = \frac{1}{J} \mathbf{e} \mathbf{e}^\top$. Then $\mathbf{\Pi}$ is an orthogonal projection, $\mathbf{V}_i \mathbf{\Pi} = \mathbf{E}[\mathbf{v}_i^{(1:J)}]$, and $\mathbf{\Gamma}_i = \frac{1}{J-1} \mathbf{V}_i (\mathbf{I} - \mathbf{\Pi}) \mathbf{V}_i^\top$, so that $\text{Ran}(\mathbf{\Gamma}_i) = \text{Ran}(\mathbf{V}_i (\mathbf{I} - \mathbf{\Pi}))$. Write $\mathbf{Y}_i = [\mathbf{y}_i^{(1)}, \mathbf{y}_i^{(2)}, \dots, \mathbf{y}_i^{(J)}] \in \mathbb{R}^{d \times J}$ and express the EKI update (3.1) as $\mathbf{V}_{i+1} = \mathbf{V}_i + \mathbf{\Gamma}_i \mathbf{H}^\top (\mathbf{H} \mathbf{\Gamma}_i \mathbf{H}^\top + \mathbf{\Sigma})^{-1} (\mathbf{Y}_i - \mathbf{H} \mathbf{V}_i)$. Postmultiplying by $(\mathbf{I} - \mathbf{\Pi})$ leads to the first conclusion:

$$\text{Ran}(\mathbf{\Gamma}_{i+1}) = \text{Ran}(\mathbf{V}_{i+1} (\mathbf{I} - \mathbf{\Pi})) \subset \text{Ran}(\mathbf{V}_i (\mathbf{I} - \mathbf{\Pi})) = \text{Ran}(\mathbf{\Gamma}_i) \subset \text{Ran}(\mathbf{V}_i).$$

Postmultiplying instead by $\mathbf{\Pi}$ leads to $\mathbf{E}[\mathbf{v}_{i+1}^{(1:J)}] = \mathbf{V}_{i+1} \mathbf{\Pi} \in \text{Ran}(\mathbf{V}_i)$, so we have

$$\mathbf{v}_{i+1}^{(j)} \in \mathbf{E}[\mathbf{v}_i^{(1:J)}] + \text{Ran}(\mathbf{\Gamma}_i) \subset \text{Ran}(\mathbf{V}_i),$$

which yields the second conclusion. □

Remark 3.11. *Note that Proposition 3.10 holds for both the deterministic and stochastic versions of basic EKI (Algorithm 1), although the remainder of this section focuses solely on the deterministic case.*

Denote by $\omega_i^{(j)} = \mathbf{v}_i^{(j)} - \mathbf{v}^*$ the residual between the j th particle and the minimum-norm least squares solution (2.1). We now show an evolution map for this residual.

Proposition 3.12. *For $i \geq 0$, $\omega_{i+1}^{(j)} = \mathbb{M}_i \omega_i^{(j)}$ with $\mathbb{M}_i = (\mathbf{I} + \Gamma_i \mathbf{H}^\top \Sigma^{-1} \mathbf{H})^{-1}$.*

Proof. Let $\mathbf{r} = \mathbf{H}\mathbf{v}^* - \mathbf{y}$ denote the least squares misfit and note that $\mathbf{r} \in \text{Ker}(\mathbf{H}^\top \Sigma^{-1})$. Then, subtracting \mathbf{v}^* from the EKI update yields

$$\omega_{i+1}^{(j)} = \mathbf{v}_{i+1}^{(j)} - \mathbf{v}^* = (\mathbf{I} - \mathbf{K}_i \mathbf{H}) \mathbf{v}_i^{(j)} - \mathbf{v}^* + \mathbf{K}_i \mathbf{y} = (\mathbf{I} - \mathbf{K}_i \mathbf{H}) (\mathbf{v}_i^{(j)} - \mathbf{v}^*) - \mathbf{K}_i \mathbf{r}.$$

We show $\mathbf{K}_i \mathbf{r} = \mathbf{0}$ and $(\mathbf{I} - \mathbf{K}_i \mathbf{H}) = \mathbb{M}_i$. First, observe that

$$\begin{aligned} (\mathbf{I} - \mathbf{K}_i \mathbf{H}) \Gamma_i \mathbf{H}^\top \Sigma^{-1} &= \Gamma_i \mathbf{H}^\top \Sigma^{-1} - \Gamma_i \mathbf{H}^\top (\mathbf{H} \Gamma_i \mathbf{H}^\top + \Sigma)^{-1} \mathbf{H} \Gamma_i \mathbf{H}^\top \Sigma^{-1} \\ &= \Gamma_i \mathbf{H}^\top (\mathbf{I} - (\mathbf{H} \Gamma_i \mathbf{H}^\top + \Sigma)^{-1} \mathbf{H} \Gamma_i \mathbf{H}^\top) \Sigma^{-1} \\ &= \Gamma_i \mathbf{H}^\top (\mathbf{H} \Gamma_i \mathbf{H}^\top + \Sigma)^{-1} = \mathbf{K}_i, \end{aligned}$$

which makes it evident that $\text{Ker}(\mathbf{H}^\top \Sigma^{-1}) \subset \text{Ker}(\mathbf{K}_i)$, so $\mathbf{K}_i \mathbf{r} = \mathbf{0}$. Finally note that the above calculation implies $\mathbf{K}_i \mathbf{H} (\mathbf{I} + \Gamma_i \mathbf{H}^\top \Sigma^{-1} \mathbf{H}) = \Gamma_i \mathbf{H}^\top \Sigma^{-1} \mathbf{H}$ which we can rearrange to $\mathbf{K}_i \mathbf{H} = \Gamma_i \mathbf{H}^\top \Sigma^{-1} \mathbf{H} \mathbb{M}_i = \mathbf{I} - \mathbb{M}_i$, so $(\mathbf{I} - \mathbf{K}_i \mathbf{H}) = \mathbb{M}_i$. \square

3.2.2 Deterministic EKI: Decomposition of state space \mathbb{R}^d

A spectral analysis of \mathbb{M}_i will distinguish three fundamental subspaces of the state space \mathbb{R}^d that are invariant under \mathbb{M}_i . Consider the following eigenvalue problem:

$$\Gamma_i \mathbf{H}^\top \Sigma^{-1} \mathbf{H} \mathbf{u}_{\ell,i} = \delta'_{\ell,i} \mathbf{u}_{\ell,i}, \quad \ell = 1, \dots, d. \quad (3.4)$$

The state space eigenpairs $(\delta'_{\ell,i}, \mathbf{u}_{\ell,i})$ of (3.4) will be seen to be closely related to the observation space eigenpairs $(\delta_{\ell,i}, \mathbf{w}_\ell)$ of (3.3):

Proposition 3.13. *Let $\{\mathbf{w}_\ell\}_{\ell=1}^n$ denote eigenvectors of (3.3) ordered as described in Proposition 3.2, and recall that the leading r eigenvectors correspond to positive eigenvalues $\delta_{\ell,i}$. For $\ell = 1, \dots, r$, define $\mathbf{u}_\ell = \frac{1}{\delta_{\ell,i}} \Gamma_i \mathbf{H}^\top \mathbf{w}_\ell$. If $h \equiv \text{rank}(\mathbf{H}) > r$, then for $\ell = r+1, \dots, h$, define $\mathbf{u}_\ell = \mathbf{H}^+ \Sigma \mathbf{w}_\ell$. Then for all $\ell \leq h$, \mathbf{u}_ℓ is an eigenvector of (3.4) with eigenvalue $\delta'_{\ell,i} = \delta_{\ell,i}$. Conversely, for all $\ell \leq h$, $\mathbf{w}_\ell = \Sigma^{-1} \mathbf{H} \mathbf{u}_\ell$.*

Proof. One may verify the relationships between \mathbf{w}_ℓ and \mathbf{u}_ℓ by direct substitution, recalling that $\mathbf{H} \mathbf{H}^+$ is the Σ^{-1} -orthogonal projection onto $\text{Ran}(\mathbf{H})$ and that for $\ell \leq h$, $\mathbf{w}_\ell \in \text{Ran}(\Sigma^{-1} \mathbf{H})$ or equivalently, $\Sigma \mathbf{w}_\ell \in \text{Ran}(\mathbf{H})$. We need still to confirm that the eigenvectors \mathbf{u}_ℓ are constant with respect to the iteration index, i . Recalling $\mathbb{M}_i = (\mathbf{I} - \mathbf{K}_i \mathbf{H})$ and assuming $(\delta'_{\ell,i}, \mathbf{u}_\ell)$ satisfies (3.4), we have

$$\begin{aligned} \Gamma_{i+1} \mathbf{H}^\top \Sigma^{-1} \mathbf{H} \mathbf{u}_\ell &= (\mathbf{I} - \mathbf{K}_i \mathbf{H}) \Gamma_i (\mathbf{I} - \mathbf{K}_i \mathbf{H})^\top \mathbf{H}^\top \Sigma^{-1} \mathbf{H} \mathbf{u}_\ell \\ &= \mathbb{M}_i \Gamma_i (\mathbf{I} - \mathbf{H}^\top (\mathbf{H} \Gamma_i \mathbf{H}^\top + \Sigma)^{-1} \mathbf{H} \Gamma_i) \mathbf{H}^\top \Sigma^{-1} \mathbf{H} \mathbf{u}_\ell \\ &= \mathbb{M}_i (\mathbf{I} - \mathbf{K}_i \mathbf{H}) \Gamma_i \mathbf{H}^\top \Sigma^{-1} \mathbf{H} \mathbf{u}_\ell = \mathbb{M}_i^2 \delta'_{\ell,i} \mathbf{u}_\ell \\ &= (\mathbf{I} + \Gamma_i \mathbf{H}^\top \Sigma^{-1} \mathbf{H})^{-2} \delta'_{\ell,i} \mathbf{u}_\ell = \delta'_{\ell,i} / (1 + \delta'_{\ell,i})^2 \mathbf{u}_\ell = \delta'_{\ell,i+1} \mathbf{u}_\ell \end{aligned}$$

\square

Remark 3.14. *The work [12] previously provided a spectral analysis of the ensemble covariance, Γ_i , for the continuous-time limit of linear deterministic EKI. This leads to a system of differential algebraic equations describing the evolution of both the eigenvectors and eigenvalues of Γ_i . In contrast, we provide a spectral analysis of \mathbb{M}_i , the iteration map governing the evolution of the least squares residual, whose eigenvectors remain constant and whose eigenvalues satisfy the simple recurrence shown in Proposition 3.1. This enables us to define fundamental subspaces in state space which are invariant under the residual iteration map.*

Proposition 3.13 defines h state space eigenvectors of (3.4) in terms of observation space eigenvectors of (3.3) and shows them to be associated with the same eigenvalues (both zero and nonzero). Proposition 3.2 states that the remaining $n - h$ eigenvalues of (3.3) are zero. Note that (3.4) must have exactly r nonzero eigenvalues because the nonzero eigenvalues of $(\mathbf{\Gamma}_i \mathbf{H}^\top)(\mathbf{\Sigma}^{-1} \mathbf{H})$ must be identical to those of $(\mathbf{\Sigma}^{-1} \mathbf{H})(\mathbf{\Gamma}_i \mathbf{H}^\top)$, whereas zero eigenvalues of either matrix (when they exist) may vary only in multiplicity as determined by dimension (see e.g., [38, Theorem 1.3.22]). Thus, the remaining $d - h$ eigenvalues that have been left unspecified in Proposition 3.13 must also be zero.

Going forward, we will drop the notational distinction between the eigenvalues of (3.3) and of (3.4), i.e., we take $\delta'_{\ell,i} = \delta_{\ell,i}$ and constrain the eigenvalue index to $\ell = 1, 2, \dots, h$. Let $\mathbf{\Delta}_{1:h}^{(i)} = \text{diag}(\delta_{1,i}, \dots, \delta_{h,i})$ and $\mathbf{U} = [\mathbf{u}_1, \dots, \mathbf{u}_h]$. Then, $\mathbf{\Gamma}_i \mathbf{H}^\top \mathbf{\Sigma}^{-1} \mathbf{H} \mathbf{U} = \mathbf{U} \mathbf{\Delta}_{1:h}^{(i)}$, and the weighted orthonormalization $\mathbf{W}^\top \mathbf{\Sigma} \mathbf{W} = \mathbf{I}_n$ implies $\mathbf{U}^\top \mathbf{H}^\top \mathbf{\Sigma}^{-1} \mathbf{H} \mathbf{U} = \mathbf{I}_h$.

We now define the three fundamental subspaces of EKI in the state space \mathbb{R}^d as specific invariant subspaces of the iteration map for the state space residual, $\mathbb{M}_i = (\mathbf{I} + \mathbf{\Gamma}_i \mathbf{H}^\top \mathbf{\Sigma}^{-1} \mathbf{H})^{-1}$, characterized through appropriately defined spectral projectors.

Proposition 3.15. *Let $\mathbf{U}_{k:\ell} \in \mathbb{R}^{d \times (\ell - k + 1)}$ contain columns k through ℓ of \mathbf{U} . Define $\mathbb{P} = \mathbf{U}_{1:r} \mathbf{U}_{1:r}^\top (\mathbf{H}^\top \mathbf{\Sigma}^{-1} \mathbf{H})$, $\mathbb{Q} = \mathbf{U}_{r+1:h} \mathbf{U}_{r+1:h}^\top (\mathbf{H}^\top \mathbf{\Sigma}^{-1} \mathbf{H})$, and $\mathbb{N} = \mathbf{I} - \mathbb{P} - \mathbb{Q}$. Then \mathbb{P} , \mathbb{Q} , and \mathbb{N} are spectral projectors for the residual iteration map \mathbb{M}_i , i.e., $\mathbb{M}_i \mathbb{P} = \mathbb{P} \mathbb{M}_i$ and $\mathbb{P}^2 = \mathbb{P}$, with similar assertions for \mathbb{Q} and \mathbb{N} . \mathbb{P} , \mathbb{Q} , and \mathbb{N} are complementary in the sense that $\mathbb{P} \mathbb{Q} = \mathbb{Q} \mathbb{N} = \mathbb{P} \mathbb{N} = \mathbf{0}$ and $\mathbb{P} + \mathbb{Q} + \mathbb{N} = \mathbf{I}$*

Proof. The assertions $\mathbb{P}^2 = \mathbb{P}$ and $\mathbb{Q}^2 = \mathbb{Q}$ and $\mathbb{P} \mathbb{Q} = \mathbf{0}$ can be verified from their definitions and the weighted orthonormalization condition $\mathbf{U}^\top \mathbf{H}^\top \mathbf{\Sigma}^{-1} \mathbf{H} \mathbf{U} = \mathbf{I}_h$, so \mathbb{P} and \mathbb{Q} are both projectors and $\mathbb{P} + \mathbb{Q} = \mathbf{U} \mathbf{U}^\top \mathbf{H}^\top \mathbf{\Sigma}^{-1} \mathbf{H}$ is also a projector. Then, \mathbb{N} is the complementary projector to $\mathbb{P} + \mathbb{Q}$ with $\text{Ran}(\mathbb{N}) = \text{Ker}(\mathbb{P} + \mathbb{Q}) = \text{Ker}(\mathbf{H})$. Then,

$$\begin{aligned} \mathbb{M}_i^{-1} (\mathbf{U}_{1:r} (\mathbf{I} + \mathbf{\Delta}_{1:r}^{(i)})^{-1} \mathbf{U}_{1:r}^\top \mathbf{H}^\top \mathbf{\Sigma}^{-1} \mathbf{H} + \mathbb{Q} + \mathbb{N}) \\ = (\mathbf{I} + \mathbf{\Gamma}_i \mathbf{H}^\top \mathbf{\Sigma}^{-1} \mathbf{H}) (\mathbf{U}_{1:r} (\mathbf{I} + \mathbf{\Delta}_{1:r}^{(i)})^{-1} \mathbf{U}_{1:r}^\top \mathbf{H}^\top \mathbf{\Sigma}^{-1} \mathbf{H} + \mathbb{Q} + \mathbb{N}) \\ = \mathbf{U}_{1:r} \mathbf{U}_{1:r}^\top \mathbf{H}^\top \mathbf{\Sigma}^{-1} \mathbf{H} + \mathbb{Q} + \mathbb{N} = \mathbb{P} + \mathbb{Q} + \mathbb{N} = \mathbf{I}, \end{aligned}$$

so $\mathbb{M}_i = \mathbf{U}_{1:r} (\mathbf{I} + \mathbf{\Delta}_{1:r}^{(i)})^{-1} \mathbf{U}_{1:r}^\top \mathbf{H}^\top \mathbf{\Sigma}^{-1} \mathbf{H} + \mathbb{Q} + \mathbb{N}$. Using this expression for \mathbb{M}_i yields

$$\begin{aligned} \mathbb{P} \mathbb{M}_i &= \mathbf{U}_{1:r} \mathbf{U}_{1:r}^\top \mathbf{H}^\top \mathbf{\Sigma}^{-1} \mathbf{H} (\mathbf{U}_{1:r} (\mathbf{I} + \mathbf{\Delta}_{1:r}^{(i)})^{-1} \mathbf{U}_{1:r}^\top \mathbf{H}^\top \mathbf{\Sigma}^{-1} \mathbf{H} + \mathbb{Q} + \mathbb{N}) \\ &= \mathbf{U}_{1:r} (\mathbf{I} + \mathbf{\Delta}_{1:r}^{(i)})^{-1} \mathbf{U}_{1:r}^\top \mathbf{H}^\top \mathbf{\Sigma}^{-1} \mathbf{H} \\ &= (\mathbf{U}_{1:r} (\mathbf{I} + \mathbf{\Delta}_{1:r}^{(i)})^{-1} \mathbf{U}_{1:r}^\top \mathbf{H}^\top \mathbf{\Sigma}^{-1} \mathbf{H} + \mathbb{Q} + \mathbb{N}) \mathbf{U}_{1:r} \mathbf{U}_{1:r}^\top \mathbf{H}^\top \mathbf{\Sigma}^{-1} \mathbf{H} = \mathbb{M}_i \mathbb{P}. \end{aligned}$$

Similar calculations show that \mathbb{M}_i commutes with \mathbb{Q} and \mathbb{N} . □

The least squares residual can thus be divided into three components associated with the oblique projectors defined in Proposition 3.15: $\boldsymbol{\omega}_i^{(j)} = \mathbb{P} \boldsymbol{\omega}_i^{(j)} + \mathbb{Q} \boldsymbol{\omega}_i^{(j)} + \mathbb{N} \boldsymbol{\omega}_i^{(j)}$. Next, we will analyze the convergence behavior of these three residual components.

3.2.3 Deterministic EKI: Convergence analysis in state space \mathbb{R}^d

We draw on eigenvalue convergence results developed in Proposition 3.6 to prove our main result concerning the evolution of the least squares residual of the EKI particles in the state space \mathbb{R}^d .

Theorem 3.16. *For all particles $j = 1, 2, \dots, J$, the following hold:*

- (a) as $i \rightarrow \infty$, $\|\mathbb{P} \boldsymbol{\omega}_i^{(j)}\| = \mathcal{O}(i^{-\frac{1}{2}})$,
- (b) for all $i \geq 0$, $\mathbb{Q} \boldsymbol{\omega}_i^{(j)} = \mathbb{Q} \boldsymbol{\omega}_0^{(j)}$, and
- (c) for all $i \geq 0$, $\mathbb{N} \boldsymbol{\omega}_i^{(j)} = \mathbb{N} \boldsymbol{\omega}_0^{(j)}$.

Proof. The proof is analogous to that of Theorem 3.8. Let $\boldsymbol{\omega}_i^{(j)} = \mathbb{M}_{i0}\boldsymbol{\omega}_0^{(j)}$, where $\mathbb{M}_{i0} = \mathbb{M}_i\mathbb{M}_{i-1}\cdots\mathbb{M}_0$ with $\mathbb{M}_i = \mathbf{U}_{1:r}(\mathbf{I} + \boldsymbol{\Delta}_{1:r}^{(i)})^{-1}\mathbf{U}_{1:r}^\top(\mathbf{H}^\top\boldsymbol{\Sigma}^{-1}\mathbf{H}) + \mathbf{Q} + \mathbf{N}$ and $\boldsymbol{\Delta}_{1:r}^{(i)}$ denotes the diagonal matrix of the first r nonzero eigenvalues. Thus, with the earlier definition of $\mathbf{D}_{i0} = \prod_{k=0}^i(\mathbf{I} + \boldsymbol{\Delta}_{1:r}^{(k)})^{-1}$, we have

$$\mathbb{M}_{i0} = \mathbf{U}_r\mathbf{D}_{i0}\mathbf{U}_r^\top(\mathbf{H}^\top\boldsymbol{\Sigma}^{-1}\mathbf{H}) + \mathbf{Q} + \mathbf{N}$$

Thus, for all i , $\mathbf{Q}\boldsymbol{\omega}_i^{(j)} = \mathbf{Q}\mathbb{M}_{i0}\boldsymbol{\omega}_0^{(j)} = \mathbf{Q}\boldsymbol{\omega}_0^{(j)}$, $\mathbf{N}\boldsymbol{\omega}_i^{(j)} = \mathbf{N}\mathbb{M}_{i0}\boldsymbol{\omega}_0^{(j)} = \mathbf{N}\boldsymbol{\omega}_0^{(j)}$, and

$$\mathbb{P}\boldsymbol{\omega}_i^{(j)} = \mathbb{P}\mathbb{M}_{i0}\boldsymbol{\omega}_0^{(j)} = \mathbf{U}_{1:r}\mathbf{D}_{i0}\mathbf{U}_{1:r}^\top(\mathbf{H}^\top\boldsymbol{\Sigma}^{-1}\mathbf{H})\mathbb{P}\boldsymbol{\omega}_0^{(j)}.$$

Recall $\|\mathbf{D}_{i0}\| = d_{r,i}$ where $d_{r,i}$ is the largest diagonal element of \mathbf{D}_{i0} as before. Then,

$$\|\mathbb{P}\boldsymbol{\omega}_i^{(j)}\| \leq d_{r,i}\|\mathbf{U}_{1:r}\|\|\mathbf{H}^\top\boldsymbol{\Sigma}^{-1}\mathbf{H}\mathbf{U}_{1:r}\|\|\mathbb{P}\boldsymbol{\omega}_0^{(j)}\|.$$

Note that for each j , $\|\mathbf{U}_{1:r}\|\|\mathbf{H}^\top\boldsymbol{\Sigma}^{-1}\mathbf{H}\mathbf{U}_{1:r}\|\|\mathbb{P}\boldsymbol{\omega}_0^{(j)}\|$ is a constant independent of i . Since we have shown in the proof of Theorem 3.8 that $d_{r,i} = \mathcal{O}(i^{-\frac{1}{2}})$, we are done. \square

Remark 3.17. The earlier works [58, 59] decompose the state space behavior into two components corresponding to our \mathbb{P} and a complementary projector under the assumption that \mathbf{H} is one-to-one, and focus on recovery of the pre-image under \mathbf{H} of \mathbf{y} rather than the least squares solution (2.1). The work [12] assumes $\boldsymbol{\Gamma}_i$ is full rank and shows that the j th particle $\mathbf{v}_i^{(j)}$ converges to the minimizer of the least-squares objective (1.1) that is closest in the $\boldsymbol{\Gamma}_0^{-1}$ -norm to its initialization, $\mathbf{v}_0^{(j)}$. In contrast, Theorem 3.16 provides the first results describing convergence of EKI particles to the standard minimum-norm least-squares minimizer (2.1). We allow both \mathbf{H} and $\boldsymbol{\Gamma}_i$ to be rank-deficient, leading to the definition of three fundamental invariant subspaces of EKI in state space analogous to those previously defined in observation space.

4 Analysis of stochastic EKI

We now provide an analysis of linear *stochastic* EKI (Algorithm 1 with $\mathbf{y}_i^{(j)} = \mathbf{y} + \boldsymbol{\varepsilon}_i^{(j)}$). Paralleling our analysis of linear deterministic EKI from Section 3, we begin with stochastic EKI results in observation space (Section 4.1) before developing related results in state space (Section 4.2).

4.1 Stochastic EKI: Analysis in observation space \mathbb{R}^n

We begin by deriving an idealized data misfit iteration that reflects an idealized covariance update (Section 4.1.1). Section 4.1.2 then provides a spectral analysis of this idealized iteration which distinguishes three fundamental subspaces of stochastic EKI. Convergence behaviors within these subspaces are analyzed in Section 4.1.3.

4.1.1 Stochastic EKI: An idealized data misfit iteration

Recall our definition of the data misfit: $\boldsymbol{\theta}_i^{(j)} = \mathbf{H}\mathbf{v}_i^{(j)} - \mathbf{y}$ for $j \leq J$ and $i \geq 0$. In stochastic EKI, $\mathbf{y}_i^{(j)} = \mathbf{y} + \boldsymbol{\varepsilon}_i^{(j)}$ in the particle update (3.1). This yields a misfit iteration similar to (3.2) but with a forcing term arising from the stochastic perturbation $\boldsymbol{\varepsilon}_i^{(j)}$:

$$\boldsymbol{\theta}_{i+1}^{(j)} = \boldsymbol{\mathcal{M}}_i\boldsymbol{\theta}_i^{(j)} + (\mathbf{I} - \boldsymbol{\mathcal{M}}_i)\boldsymbol{\varepsilon}_i^{(j)} \quad (4.1)$$

where $\boldsymbol{\mathcal{M}}_i = \boldsymbol{\Sigma}(\mathbf{H}\boldsymbol{\Gamma}_i\mathbf{H}^\top + \boldsymbol{\Sigma})^{-1}$, defined as before. In our analysis of deterministic EKI, we showed that generalized eigenvectors of the pencil $(\mathbf{H}\boldsymbol{\Gamma}_i\mathbf{H}^\top, \boldsymbol{\Sigma})$ remain constant under the deterministic EKI iteration, enabling us to define fundamental subspaces that are invariant under $\boldsymbol{\mathcal{M}}_i$ across all iterations. This invariance no longer holds for stochastic EKI: to see this, note that under the stochastic misfit iteration (4.1), the observation space covariance $\mathbf{H}\boldsymbol{\Gamma}_i\mathbf{H}^\top = \text{cov}[\boldsymbol{\theta}_i^{(1:J)}]$ satisfies

$$\begin{aligned} \mathbf{H}\boldsymbol{\Gamma}_{i+1}\mathbf{H}^\top &= \boldsymbol{\mathcal{M}}_i\mathbf{H}\boldsymbol{\Gamma}_i\mathbf{H}^\top\boldsymbol{\mathcal{M}}_i^\top + \boldsymbol{\mathcal{M}}_i\text{cov}[\mathbf{H}\mathbf{v}_i^{(1:J)}, \boldsymbol{\varepsilon}_i^{(1:J)}](\mathbf{I} - \boldsymbol{\mathcal{M}}_i)^\top \cdots \\ &\quad + (\mathbf{I} - \boldsymbol{\mathcal{M}}_i)\text{cov}[\boldsymbol{\varepsilon}_i^{(1:J)}, \mathbf{H}\mathbf{v}_i^{(1:J)}]\boldsymbol{\mathcal{M}}_i^\top + (\mathbf{I} - \boldsymbol{\mathcal{M}}_i)\text{cov}[\boldsymbol{\varepsilon}_i^{(1:J)}](\mathbf{I} - \boldsymbol{\mathcal{M}}_i)^\top. \end{aligned} \quad (4.2)$$

Relative to its deterministic EKI analogue (cf. the proof of Proposition 3.1), eq. (4.2) has several additional terms dependent on the realizations of the stochastic perturbations $\varepsilon_i^{(j)}$ at the current iteration that will lead to eigenvectors of $(\mathbf{H}\mathbf{\Gamma}_i\mathbf{H}^\top, \mathbf{\Sigma})$ changing from one iteration to the next. Instead of carefully accounting for these changes, we will base our analytical treatment of stochastic EKI on an idealized covariance iteration which we now motivate and define.

Let $\varepsilon_{0:k}^{(1:J)} = \{\varepsilon_i^{(j)}\}_{i=0,j=1}^{k,J}$ denote the set of all stochastic perturbations through iteration k for all particles $j = 1, \dots, J$. Note that in (4.2), the quantities $\mathbf{\Gamma}_i$, $\mathbf{\mathcal{M}}_i$, and $\mathbf{v}_i^{(j)}$ are all random variables that depend on previous noise realizations $\varepsilon_{0:i-1}^{(1:J)}$. Conditioning on the previous noise and taking the expectation of (4.2) with respect to the current (i th) noise perturbations yields

$$\mathbb{E}[\mathbf{H}\mathbf{\Gamma}_{i+1}\mathbf{H}^\top | \varepsilon_{0:i-1}^{(j)}] = \mathbf{\mathcal{M}}_i\mathbf{H}\mathbf{\Gamma}_i\mathbf{H}^\top\mathbf{\mathcal{M}}_i^\top + (\mathbf{I} - \mathbf{\mathcal{M}}_i)\mathbf{\Sigma}(\mathbf{I} - \mathbf{\mathcal{M}}_i)^\top,$$

which, after substitution and some rearrangement becomes

$$\mathbb{E}[\mathbf{H}\mathbf{\Gamma}_{i+1}\mathbf{H}^\top | \varepsilon_{0:i-1}^{(j)}] = \mathbf{\Sigma} - \mathbf{\Sigma}(\mathbf{H}\mathbf{\Gamma}_i\mathbf{H}^\top + \mathbf{\Sigma})^{-1}\mathbf{\Sigma}. \quad (4.3)$$

This motivates the definition of $\mathbf{C}_i \in \mathbb{R}^{n \times n}$ for $i \geq 0$ as follows:

$$\mathbf{C}_0 = \mathbf{H}\mathbf{\Gamma}_0\mathbf{H}^\top \quad \text{and} \quad \mathbf{C}_{i+1} = \mathbf{\Sigma} - \mathbf{\Sigma}(\mathbf{C}_i + \mathbf{\Sigma})^{-1}\mathbf{\Sigma}, \quad \text{for } i \geq 0. \quad (4.4)$$

The matrices \mathbf{C}_i satisfy an *idealized covariance iteration* (4.4) reflecting the form of the conditional expectation (4.3), and so \mathbf{C}_i can be viewed as idealized analogues of $\mathbf{H}\mathbf{\Gamma}_i\mathbf{H}^\top$. We then define the idealized misfit iteration map $\widetilde{\mathbf{\mathcal{M}}}_i = \mathbf{\Sigma}(\mathbf{C}_i + \mathbf{\Sigma})^{-1}$, analogous to $\mathbf{\mathcal{M}}_i$, leading to the following *idealized misfit iteration* (analogous to (4.1)):

$$\tilde{\boldsymbol{\theta}}_0^{(j)} = \boldsymbol{\theta}_0^{(j)}, \quad \tilde{\boldsymbol{\theta}}_{i+1}^{(j)} = \widetilde{\mathbf{\mathcal{M}}}_i\tilde{\boldsymbol{\theta}}_i^{(j)} + (\mathbf{I} - \widetilde{\mathbf{\mathcal{M}}}_i)\varepsilon_i^{(j)}, \quad \text{for } i = 0, 1, \dots \quad (4.5)$$

In what follows, our analysis of stochastic EKI will treat this idealized misfit iteration and its state-space counterpart, which we will show share favorable properties with their deterministic EKI analogues.

Remark 4.1. We relate the analysis of our idealized iteration (4.5) to earlier works providing analyses of stochastic EKI. The works [9, 10] analyze the continuous-time limit of the stochastic iteration, yielding a system of coupled stochastic differential equations governing individual particle trajectories. In this analysis approach, the authors introduce additive covariance inflation in order to prevent the ensemble from collapsing prematurely before converging to a solution [9]. Along similar lines, we show within our framework in Proposition A.1 that $\mathbf{C}_i \geq \mathbb{E}[\mathbf{H}\mathbf{\Gamma}_i\mathbf{H}^\top]$, so that the idealized iteration (4.5) can be interpreted as reflecting an implicit inflation of covariance. We show that under (4.4), the idealized covariance \mathbf{C}_i collapses only in the infinite iteration limit. Note that by defining \mathbf{C}_i so as to reflect the conditional expectation iteration (4.3) (as opposed to explicitly adding a positive covariance inflation term), our approach enables the true stochastic EKI iteration (4.1) to be interpreted as a particle approximation of the idealized iteration (4.5). The results we prove concerning the idealized iteration therefore most closely reflect stochastic EKI behavior when the ensemble size is large, and shed light into the failure of stochastic EKI to converge when the ensemble size is small (see numerical results in Section 5). Our analysis approach therefore shares some commonalities with mean-field limit analyses of stochastic EKI [12, 26], which analyze the algorithm in the infinite ensemble limit, leading to deterministic expressions governing the ensemble statistics (mean and covariance). In contrast, while our idealized covariance iteration expression (4.4) is deterministic, we provide new expressions for the idealized misfits of individual particles (4.5) retaining the stochastic dependence on perturbations, and revealing convergence properties for individual particle paths supported by numerical experiments.

4.1.2 Stochastic EKI: Decomposition of observation space \mathbb{R}^n

We now provide a spectral analysis of $\widetilde{\mathbf{\mathcal{M}}}_i$ that distinguishes three fundamental subspaces that are invariant under (4.5). Consider the generalized eigenvalue problem

$$\mathbf{C}_i\tilde{\mathbf{w}}_{\ell,i} = \tilde{\delta}_{\ell,i}\mathbf{\Sigma}\tilde{\mathbf{w}}_{\ell,i}. \quad (4.6)$$

We now show an analogue of Proposition 3.1:

Proposition 4.2. Let $(\tilde{\delta}_i, \tilde{\mathbf{w}})$ be an eigenpair for the pencil (\mathbf{C}_i, Σ) , i.e., satisfying (4.6). Then, $\tilde{\mathbf{w}}$ is also an eigenvector of the pencil $(\mathbf{C}_{i+1}, \Sigma)$ with eigenvalue $\tilde{\delta}_{i+1} = \frac{\tilde{\delta}_i}{1+\tilde{\delta}_i}$.

Proof. From our definition (4.4) of the iteration determining \mathbf{C}_i , we have

$$\mathbf{C}_{i+1}\tilde{\mathbf{w}} = (\mathbf{I} - \Sigma(\mathbf{C}_i + \Sigma)^{-1})\Sigma\tilde{\mathbf{w}} = \mathbf{C}_i(\mathbf{C}_i + \Sigma)^{-1}\Sigma\tilde{\mathbf{w}} = \frac{\tilde{\delta}_i}{1+\tilde{\delta}_i}\Sigma\tilde{\mathbf{w}}.$$

□

As in the deterministic case we now write $\tilde{\mathbf{w}}_\ell = \tilde{\mathbf{w}}_{\ell,i}$ for all i . An analogue of Proposition 3.2 concerning the construction of an eigenvector basis for \mathbb{R}^n holds:

Proposition 4.3. $\tilde{\delta}_{\ell,0} = 0$ implies $\tilde{\delta}_{\ell,i} = 0$ for all $i \geq 1$; and $\tilde{\delta}_{\ell,0} > 0$ implies $\tilde{\delta}_{\ell,i} > 0$ for all $i \geq 1$. Let r denote the number of positive eigenvalues of (4.6). There is a Σ -orthogonal basis for \mathbb{R}^n comprised of eigenvectors of (4.6), $\{\tilde{\mathbf{w}}_1, \dots, \tilde{\mathbf{w}}_n\}$, satisfying

1. $\{\tilde{\mathbf{w}}_1, \dots, \tilde{\mathbf{w}}_r\} \subset \text{Ran}(\Sigma^{-1}\mathbf{H})$ are eigenvectors of (4.6) associated with positive eigenvalues $\delta_{1,i}, \dots, \delta_{r,i}$, labeled in non-increasing order at $i = 1$, that is, $\tilde{\delta}_{1,1} \geq \tilde{\delta}_{2,1} \geq \dots \geq \tilde{\delta}_{r,1} > 0$. This ordering is preserved for subsequent $i \geq 1$.
2. if $r < h$, $\{\tilde{\mathbf{w}}_{r+1}, \dots, \tilde{\mathbf{w}}_h\} \subset \text{Ran}(\Sigma^{-1}\mathbf{H})$ are eigenvectors of (4.6) associated with zero eigenvalues, and
3. if $h < n$, $\{\tilde{\mathbf{w}}_{h+1}, \dots, \tilde{\mathbf{w}}_n\} \subset \text{Ker}(\mathbf{H}^\top)$ are eigenvectors of (4.6) also associated with zero eigenvalues.

The proof is analogous to that of Proposition 3.2.

Let $\tilde{\mathbf{W}} = [\tilde{\mathbf{w}}_1, \dots, \tilde{\mathbf{w}}_n]$, with the normalization $\tilde{\mathbf{W}}^\top \Sigma \tilde{\mathbf{W}} = \mathbf{I}$. We define spectral projectors of $\tilde{\mathcal{M}}_i$ that divide \mathbb{R}^n into three fundamental subspaces of stochastic EKI:

Proposition 4.4. Let $\tilde{\mathbf{W}}_{k:\ell} \in \mathbb{R}^{n \times (\ell-k+1)}$ denote the k -through- ℓ -th columns of $\tilde{\mathbf{W}}$. Define $\tilde{\mathcal{P}} = \Sigma \tilde{\mathbf{W}}_{1:r} \tilde{\mathbf{W}}_{1:r}^\top$, $\tilde{\mathcal{Q}} = \Sigma \tilde{\mathbf{W}}_{r+1:h} \tilde{\mathbf{W}}_{r+1:h}^\top$, and $\tilde{\mathcal{N}} = \Sigma \tilde{\mathbf{W}}_{h+1:n} \tilde{\mathbf{W}}_{h+1:n}^\top$. Then, $\tilde{\mathcal{P}}$, $\tilde{\mathcal{Q}}$, and $\tilde{\mathcal{N}}$ are complementary spectral projectors associated with the idealized misfit iteration map $\tilde{\mathcal{M}}_i$.

The proof is essentially the same as that of Proposition 3.3.

As in the deterministic case, the spectral projectors $\tilde{\mathcal{P}}$, $\tilde{\mathcal{Q}}$, and $\tilde{\mathcal{N}}$ decompose the idealized misfit $\tilde{\theta}_i^{(j)}$ into three components exhibiting differing convergence behaviors, which we characterize in the next section.

4.1.3 Stochastic EKI: Convergence analysis in observation space \mathbb{R}^n

We begin by showing that the positive eigenvalues of (4.6) decay at a $1/i$ rate:

Corollary 4.5. If $\tilde{\delta}_{\ell,0} > 0$, then for all i , $\tilde{\delta}_{\ell,i} = (\frac{1}{\tilde{\delta}_{\ell,0}} + i)^{-1}$.

Proof. The proof follows by induction with the base case $i = 1$ established directly from Proposition 4.2. □

We now turn our attention to the behavior of the idealized misfit $\tilde{\theta}_i^{(j)}$ as $i \rightarrow \infty$. Let $\tilde{\mathcal{M}}_{ik} = \prod_{j=k}^i \tilde{\mathcal{M}}_j$. Note that (4.5) implies

$$\tilde{\theta}_{i+1}^{(j)} = \tilde{\mathcal{M}}_{i0} \tilde{\theta}_0^{(j)} + (\mathbf{I} - \tilde{\mathcal{M}}_i) \varepsilon_i^{(j)} + \sum_{k=0}^{i-1} \tilde{\mathcal{M}}_{i,k+1} (\mathbf{I} - \tilde{\mathcal{M}}_k) \varepsilon_k^{(j)}. \quad (4.7)$$

We first show a lemma expressing the operators $\tilde{\mathcal{M}}_{ik}$ and $(\mathbf{I} - \tilde{\mathcal{M}}_i)$ in terms of eigenvectors and eigenvalues of (4.6):

Lemma 4.6. The following hold:

$$\mathbf{I} - \tilde{\mathcal{M}}_i = \sum_{\ell=1}^r \tilde{\delta}_{\ell,i+1} \Sigma \tilde{\mathbf{w}}_\ell \tilde{\mathbf{w}}_\ell^\top; \quad \tilde{\mathcal{M}}_{ik} = \sum_{\ell=1}^r \frac{\tilde{\delta}_{\ell,i+1}}{\tilde{\delta}_{\ell,k}} \Sigma \tilde{\mathbf{w}}_\ell \tilde{\mathbf{w}}_\ell^\top + \tilde{\mathcal{Q}} + \tilde{\mathcal{N}}. \quad (4.8)$$

Proof. Note that $\widetilde{\mathcal{M}}_i = \Sigma \widetilde{\mathbf{W}} (\mathbf{I} + \widetilde{\Delta}_i)^{-1} \widetilde{\mathbf{W}}^\top$, so

$$\widetilde{\mathcal{M}}_i = \sum_{\ell=1}^n \frac{1}{1 + \widetilde{\delta}_{\ell,i}} \Sigma \widetilde{\mathbf{w}}_\ell \widetilde{\mathbf{w}}_\ell^\top = \sum_{\ell=1}^r \frac{1}{1 + \widetilde{\delta}_{\ell,i}} \Sigma \widetilde{\mathbf{w}}_\ell \widetilde{\mathbf{w}}_\ell^\top + \widetilde{\mathcal{Q}} + \widetilde{\mathcal{N}}.$$

Thus,

$$\mathbf{I} - \widetilde{\mathcal{M}}_i = \sum_{\ell=1}^r \frac{\widetilde{\delta}_{\ell,i}}{1 + \widetilde{\delta}_{\ell,i}} \Sigma \widetilde{\mathbf{w}}_\ell \widetilde{\mathbf{w}}_\ell^\top, \quad \widetilde{\mathcal{M}}_{ik} = \sum_{\ell=1}^r \left(\prod_{j=k}^i \frac{1}{1 + \widetilde{\delta}_{\ell,j}} \right) \Sigma \widetilde{\mathbf{w}}_\ell \widetilde{\mathbf{w}}_\ell^\top + \widetilde{\mathcal{Q}} + \widetilde{\mathcal{N}}.$$

Recall from proposition 4.2 that $\widetilde{\delta}_{\ell,i+1} = \frac{\widetilde{\delta}_{\ell,i}}{1 + \widetilde{\delta}_{\ell,i}}$, which implies $\frac{1}{1 + \widetilde{\delta}_{\ell,i}} = \frac{\widetilde{\delta}_{\ell,i+1}}{\widetilde{\delta}_{\ell,i}}$. Substituting these relationships into the above expression yields the desired claims. \square

Our main result concerns the convergence of the idealized misfit iteration (4.5).

Theorem 4.7. *For all particles $j = 1, 2, \dots, J$, the following hold:*

- (a) *as $i \rightarrow \infty$, $\mathbb{E}[\|\widetilde{\mathcal{P}}\widetilde{\theta}_i^{(j)}\|] = \mathcal{O}(i^{-\frac{1}{2}})$,*
- (b) *for all $i \geq 0$, $\widetilde{\mathcal{Q}}\widetilde{\theta}_i^{(j)} = \widetilde{\mathcal{Q}}\widetilde{\theta}_0^{(j)}$, and*
- (c) *for all $i \geq 0$, $\widetilde{\mathcal{N}}\widetilde{\theta}_i^{(j)} = \widetilde{\mathcal{N}}\widetilde{\theta}_0^{(j)}$.*

Proof. For all i , $\widetilde{\mathcal{Q}}$ is a spectral projector of $\widetilde{\mathcal{M}}_i$ (Proposition 4.4) and $\text{Ran}(\widetilde{\mathcal{Q}}) \subset \text{Ker}(\mathbf{I} - \widetilde{\mathcal{M}}_i)$ (Lemma 4.6). Thus, applying $\widetilde{\mathcal{Q}}$ to (4.7) yields:

$$\widetilde{\mathcal{Q}}\widetilde{\theta}_{i+1}^{(j)} = \widetilde{\mathcal{M}}_{i0}\widetilde{\mathcal{Q}}\widetilde{\theta}_0^{(j)} = \widetilde{\mathcal{Q}}\widetilde{\theta}_0^{(j)} \quad \text{for all } i,$$

which gives (b). The same argument holds for $\widetilde{\mathcal{N}}\widetilde{\theta}_i^{(j)}$, which gives (c). To show (a), note that (4.7) and Lemma 4.6 for $i \geq 1$ leads to:

$$\widetilde{\mathcal{P}}\widetilde{\theta}_i^{(j)} = \sum_{\ell=1}^r \frac{\widetilde{\delta}_{\ell,i}}{\widetilde{\delta}_{\ell,0}} \Sigma \widetilde{\mathbf{w}}_\ell \widetilde{\mathbf{w}}_\ell^\top \left(\widetilde{\mathcal{P}}\widetilde{\theta}_0^{(j)} \right) + \sum_{\ell=1}^r \widetilde{\delta}_{\ell,i} \Sigma \widetilde{\mathbf{w}}_\ell \widetilde{\mathbf{w}}_\ell^\top \left(\sum_{k=0}^{i-1} \varepsilon_k^{(j)} \right).$$

Let $c_\ell = \frac{1}{\widetilde{\delta}_{\ell,0}}$. Then, from Corollary 4.5 we have:

$$\widetilde{\mathcal{P}}\widetilde{\theta}_i^{(j)} = \sum_{\ell=1}^r \frac{c_\ell}{i + c_\ell} \Sigma \widetilde{\mathbf{w}}_\ell \widetilde{\mathbf{w}}_\ell^\top \left(\widetilde{\mathcal{P}}\widetilde{\theta}_0^{(j)} \right) + \sum_{\ell=1}^r \frac{1}{i + c_\ell} \Sigma \widetilde{\mathbf{w}}_\ell \widetilde{\mathbf{w}}_\ell^\top \left(\sum_{k=0}^{i-1} \varepsilon_k^{(j)} \right),$$

so that

$$\mathbb{E}[\widetilde{\mathcal{P}}\widetilde{\theta}_i^{(j)}] = \sum_{\ell=1}^r \frac{c_\ell}{i + c_\ell} \Sigma \widetilde{\mathbf{w}}_\ell \widetilde{\mathbf{w}}_\ell^\top \left(\widetilde{\mathcal{P}}\widetilde{\theta}_0^{(j)} \right) \quad \text{and} \quad \text{Cov}(\widetilde{\mathcal{P}}\widetilde{\theta}_i^{(j)}) = \sum_{\ell=1}^r \frac{i}{(i + c_\ell)^2} \Sigma \widetilde{\mathbf{w}}_\ell \widetilde{\mathbf{w}}_\ell^\top \Sigma.$$

Using Jensen's inequality and noting $\text{trace}(\Sigma \widetilde{\mathbf{w}}_\ell \widetilde{\mathbf{w}}_\ell^\top \Sigma) = \widetilde{\mathbf{w}}_\ell^\top \Sigma^{\frac{1}{2}} \Sigma \Sigma^{\frac{1}{2}} \widetilde{\mathbf{w}}_\ell \leq \|\Sigma\|$,

$$\mathbb{E}[\|\widetilde{\mathcal{P}}\widetilde{\theta}_i^{(j)}\|^2] \leq \mathbb{E}[\|\widetilde{\mathcal{P}}\widetilde{\theta}_i^{(j)}\|^2] \leq \text{trace}(\text{Cov}(\widetilde{\mathcal{P}}\widetilde{\theta}_i^{(j)})) \leq \|\Sigma\| \sum_{\ell=1}^r \frac{i}{(i + c_\ell)^2} \leq \|\Sigma\| \left(\frac{r}{i} \right), \quad (4.9)$$

which is $\mathcal{O}(i^{-1})$, as $i \rightarrow \infty$. This gives the conclusion for (a). \square

Remark 4.8. Theorem 4.7 shows that our characterization of EKI's differing convergence behaviors in its fundamental subspaces carries over from deterministic EKI (Theorem 3.8) to stochastic EKI. This understanding of stochastic EKI convergence is new: while the work [12] showed that convergence of the ensemble mean under the mean-field limit can be characterized in terms of two subspaces under the assumption that $\mathbf{\Gamma}_i$ is full rank, Theorem 4.7 generalizes to allow low rank $\mathbf{\Gamma}_i$ and provides a decomposition of the convergence behaviors of individual particles under the idealized iteration (4.5). We note that while Theorem 4.7 shows convergence of the expected norm of the observable populated component $\tilde{\mathcal{P}}\tilde{\boldsymbol{\theta}}_i^{(j)}$, stronger conclusions can be drawn. Indeed, the proof of Theorem 4.7 shows that $\tilde{\mathcal{P}}\tilde{\boldsymbol{\theta}}_i^{(j)} \rightarrow \mathbf{0}$ in the mean-square sense. We show in the appendix that $\|\tilde{\mathcal{P}}\tilde{\boldsymbol{\theta}}_i^{(j)}\| \rightarrow 0$ in probability at a rate that can be made arbitrarily close to $1/\sqrt{i}$ and that in the $i \rightarrow \infty$ limit, $\tilde{\mathcal{P}}\tilde{\boldsymbol{\theta}}_i^{(j)}$ converges to zero almost surely.

4.2 Stochastic EKI: Analysis in state space \mathbb{R}^d

We now analyze the behavior of the particles $\mathbf{v}_i^{(j)}$ in the state space \mathbb{R}^d . In Section 4.2.1, we define an idealized residual iteration (the state-space counterpart to the idealized misfit iteration from Section 4.1.1). We provide a spectral analysis of this iteration and definitions of the fundamental subspaces in Section 4.2.2, and prove convergence in Section 4.2.3.

4.2.1 Stochastic EKI: An idealized least-squares residual iteration

We again consider the state space residual of the j th particle at the i th iteration: $\boldsymbol{\omega}_i^{(j)} = \mathbf{v}_i^{(j)} - \mathbf{v}^*$. Under the stochastic update equation of Algorithm 1, the state space residual satisfies:

$$\boldsymbol{\omega}_{i+1}^{(j)} = \mathbb{M}_i \boldsymbol{\omega}_i^{(j)} + \mathbf{K}_i \boldsymbol{\varepsilon}_i^{(j)}, \quad (4.10)$$

where $\mathbb{M}_i = (\mathbf{I} + \mathbf{\Gamma}_i \mathbf{H}^\top \boldsymbol{\Sigma}^{-1} \mathbf{H})^{-1}$ and $\mathbf{K}_i = \mathbf{\Gamma}_i \mathbf{H}^\top (\mathbf{H} \mathbf{\Gamma}_i \mathbf{H}^\top + \boldsymbol{\Sigma})^{-1}$ as before. Note that $\mathbb{M}_i = \mathbf{I} - \mathbf{K}_i \mathbf{H}$. Consider the evolution of the empirical particle covariance $\mathbf{\Gamma}_i \equiv \text{cov}[\mathbf{v}_i^{(1:J)}]$. We take the expectation of $\mathbf{\Gamma}_{i+1}$ conditioned on previously applied perturbations $\boldsymbol{\varepsilon}_{0:i-1}^{(1:J)}$ (analogous to (4.3)):

$$\mathbb{E}[\mathbf{\Gamma}_{i+1} | \boldsymbol{\varepsilon}_{0:i-1}^{(1:J)}] = \mathbb{M}_i \mathbf{\Gamma}_i \mathbb{M}_i^\top + \mathbf{K}_i \boldsymbol{\Sigma} \mathbf{K}_i^\top = \mathbf{\Gamma}_i - \mathbf{\Gamma}_i \mathbf{H}^\top (\mathbf{H} \mathbf{\Gamma}_i \mathbf{H}^\top + \boldsymbol{\Sigma})^{-1} \mathbf{H} \mathbf{\Gamma}_i = \mathbb{M}_i \mathbf{\Gamma}_i.$$

In what follows, we define

$$\mathbf{G}_0 = \mathbf{\Gamma}_0 \quad \text{and} \quad \mathbf{G}_{i+1} = \tilde{\mathbb{M}}_i \mathbf{G}_i, \quad \text{with} \quad \tilde{\mathbb{M}}_i = (\mathbf{I} + \mathbf{G}_i \mathbf{H}^\top \boldsymbol{\Sigma}^{-1} \mathbf{H})^{-1}. \quad (4.11)$$

We now define $\tilde{\mathbf{K}}_i = \mathbf{G}_i \mathbf{H}^\top (\mathbf{H} \mathbf{G}_i \mathbf{H}^\top + \boldsymbol{\Sigma})^{-1}$ and consider the iteration:

$$\tilde{\boldsymbol{\omega}}_0^{(j)} = \boldsymbol{\omega}_0^{(j)}, \quad \tilde{\boldsymbol{\omega}}_{i+1}^{(j)} = \tilde{\mathbb{M}}_i \tilde{\boldsymbol{\omega}}_i^{(j)} + \tilde{\mathbf{K}}_i \boldsymbol{\varepsilon}_i^{(j)}. \quad (4.12)$$

One may verify that (4.11) leads to (4.4) with $\mathbf{C}_i = \mathbf{H} \mathbf{G}_i \mathbf{H}^\top$. The expression (4.12) is therefore a state-space analogue of the idealized iteration (4.5) in the observation space. The true least squares residual iteration (4.10) can then be interpreted as a finite-ensemble approximation to the idealized iteration (4.12).

4.2.2 Stochastic EKI: Decomposition of state space \mathbb{R}^d

To analyze the convergence of the idealized state space residual iteration (4.12), we consider the following eigenvalue problem:

$$\mathbf{G}_i \mathbf{H}^\top \boldsymbol{\Sigma}^{-1} \mathbf{H} \tilde{\mathbf{u}}_{\ell,i} = \tilde{\delta}'_{\ell,i} \tilde{\mathbf{u}}_{\ell,i}. \quad (4.13)$$

We now show that the eigenvectors of (4.13) are constant and that the eigenvalues satisfy a simple recurrence relation:

Proposition 4.9. Let $\{\tilde{\mathbf{w}}_\ell\}_{\ell=1}^n$ denote eigenvectors of (4.6) ordered as described in Proposition 4.3, and recall that the leading r eigenvectors correspond to positive $\tilde{\delta}_{\ell,i}$. For $\ell = 1, \dots, r$, define $\tilde{\mathbf{u}}_\ell = \frac{1}{\tilde{\delta}_{\ell,i}} \mathbf{G}_i \mathbf{H}^\top \tilde{\mathbf{w}}_\ell$. Then, for all $\ell \leq h$, $\tilde{\mathbf{u}}_\ell$ is an eigenvector of (4.13) with eigenvalue $\tilde{\delta}'_{\ell,i} = \tilde{\delta}_{\ell,i}$. Conversely, for all $\ell \leq h$, $\tilde{\mathbf{w}}_\ell = \Sigma^{-1} \mathbf{H} \tilde{\mathbf{u}}_\ell$.

The proof is analogous to that of Proposition 3.13. Going forward we now drop the notational distinction between eigenvalues of (4.6) and of (4.13), taking $\tilde{\delta}'_{\ell,i} = \tilde{\delta}_{\ell,i}$ and constraining the eigenvalue index to $\ell \leq h$. We can now define spectral projectors of the idealized state-space residual iteration map $\tilde{\mathbb{M}}_i$:

Proposition 4.10. Let $\tilde{\mathbf{U}}_{k:\ell} \in \mathbb{R}^{d \times (\ell-k+1)}$ denote the k -through- ℓ th columns of $\tilde{\mathbf{U}}$. Define $\tilde{\mathbb{P}} = \tilde{\mathbf{U}}_{1:r} \tilde{\mathbf{U}}_{1:r}^\top \mathbf{H}^\top \Sigma^{-1} \mathbf{H}$, $\tilde{\mathbb{Q}} = \tilde{\mathbf{U}}_{r+1:h} \tilde{\mathbf{U}}_{r+1:h}^\top \mathbf{H}^\top \Sigma^{-1} \mathbf{H}$, and $\tilde{\mathbb{N}} = \mathbf{I} - \tilde{\mathbb{P}} - \tilde{\mathbb{Q}}$. Then, $\tilde{\mathbb{P}}$, $\tilde{\mathbb{Q}}$, and $\tilde{\mathbb{N}}$ are spectral projectors associated with $\tilde{\mathbb{M}}_i$.

The proof is the same as that of Proposition 3.15.

4.2.3 Stochastic EKI: Convergence analysis in state space \mathbb{R}^d

We now consider the behavior of the state space residual $\tilde{\omega}_i^{(j)}$ as $i \rightarrow \infty$. Let $\tilde{\mathbb{M}}_{ik} = \prod_{j=k}^i \tilde{\mathbb{M}}_j$. Note that (4.12) implies:

$$\tilde{\omega}_{i+1}^{(j)} = \tilde{\mathbb{M}}_{i0} \tilde{\omega}_0^{(j)} + \tilde{\mathbf{K}}_i \boldsymbol{\varepsilon}_i^{(j)} + \sum_{k=0}^{i-1} \tilde{\mathbb{M}}_{i,k+1} \tilde{\mathbf{K}}_k \boldsymbol{\varepsilon}_k^{(j)}. \quad (4.14)$$

We first show a lemma expressing $\tilde{\mathbb{M}}_{ik}$ and $\tilde{\mathbf{K}}_i$ in terms of the spectral projectors defined in Proposition 4.10 and the eigenvectors of (4.13) and (4.6).

Lemma 4.11. *The following hold:*

$$\tilde{\mathbb{M}}_{ik} = \sum_{\ell=1}^r \frac{\tilde{\delta}_{\ell,i+1}}{\tilde{\delta}_{\ell,k}} \tilde{\mathbf{u}}_\ell \tilde{\mathbf{u}}_\ell^\top \mathbf{H}^\top \Sigma^{-1} \mathbf{H} + \tilde{\mathbb{Q}} + \tilde{\mathbb{N}}, \quad \tilde{\mathbf{K}}_i = \sum_{\ell=1}^r \tilde{\delta}_{\ell,i+1} \tilde{\mathbf{u}}_\ell \tilde{\mathbf{w}}_\ell^\top. \quad (4.15)$$

Proof. The fact that $\tilde{\mathbb{M}}_i = \sum_{\ell=1}^r \frac{1}{1+\tilde{\delta}_{\ell,i}} \tilde{\mathbf{u}}_\ell \tilde{\mathbf{u}}_\ell^\top \mathbf{H}^\top \Sigma^{-1} \mathbf{H} + \tilde{\mathbb{Q}} + \tilde{\mathbb{N}}$ can be verified directly by multiplying out the given expression with $\tilde{\mathbb{M}}_i^{-1} = \mathbf{I} + \mathbf{G}_i \mathbf{H}^\top \Sigma^{-1} \mathbf{H}$ (see the similar calculation in the proof of Proposition 3.13). To obtain the expression for $\tilde{\mathbf{K}}_i$, recall $\tilde{\mathbf{K}}_i \mathbf{H} = (\mathbf{I} - \tilde{\mathbb{M}}_i)$, and that $\tilde{\mathbf{w}}_\ell = \Sigma^{-1} \mathbf{H} \tilde{\mathbf{u}}_\ell$ for $\ell \leq r \leq h$ (from Proposition 4.9), and that $\frac{1}{1+\tilde{\delta}_{\ell,i}} = \frac{\tilde{\delta}_{\ell,i+1}}{\tilde{\delta}_{\ell,i}}$. Next,

$$\tilde{\mathbb{M}}_{ik} = \sum_{\ell=1}^r \prod_{j=k}^i \frac{\tilde{\delta}_{\ell,j+1}}{\tilde{\delta}_{\ell,j}} \tilde{\mathbf{u}}_\ell \tilde{\mathbf{u}}_\ell^\top \mathbf{H}^\top \Sigma^{-1} \mathbf{H} + \tilde{\mathbb{Q}} + \tilde{\mathbb{N}}.$$

Noting that $\prod_{j=k}^i \frac{\tilde{\delta}_{\ell,j+1}}{\tilde{\delta}_{\ell,j}} = \frac{\tilde{\delta}_{\ell,i+1}}{\tilde{\delta}_{\ell,k}}$ yields the result. \square

We can now prove our main result.

Theorem 4.12. *For all particles $j = 1, 2, \dots, J$, the following hold:*

- (a) as $i \rightarrow \infty$, $\mathbb{E}[\|\tilde{\mathbb{P}} \tilde{\omega}_i^{(j)}\|] = \mathcal{O}(i^{-\frac{1}{2}})$,
- (b) for all $i \geq 0$, $\tilde{\mathbb{Q}} \tilde{\omega}_i^{(j)} = \tilde{\mathbb{Q}} \tilde{\omega}_0^{(j)}$, and
- (c) for all $i \geq 0$, $\tilde{\mathbb{N}} \tilde{\omega}_i^{(j)} = \tilde{\mathbb{N}} \tilde{\omega}_0^{(j)}$.

Proof. The argument for statements (b) and (c) is essentially the same as the argument for statements (b) and (c) of Theorem 4.7. For (a): we apply \mathbb{P} to $\tilde{\omega}_i^{(j)}$ (4.14) and substitute our expressions from Lemma 4.11 to obtain:

$$\begin{aligned}\tilde{\mathbb{P}}\tilde{\omega}_i^{(j)} &= \sum_{\ell=1}^r \frac{\tilde{\delta}_{\ell,i}}{\tilde{\delta}_{\ell,0}} \tilde{\mathbf{u}}_\ell \tilde{\mathbf{u}}_\ell^\top \mathbf{H}^\top \Sigma^{-1} \mathbf{H} \tilde{\omega}_0^{(j)} + \sum_{k=0}^{i-1} \sum_{\ell=1}^r \tilde{\delta}_{\ell,i} \tilde{\mathbf{u}}_\ell \tilde{\mathbf{w}}_\ell^\top \boldsymbol{\varepsilon}_k^{(j)} \\ &= \sum_{\ell=1}^r \frac{c_\ell}{i + c_\ell} \tilde{\mathbf{u}}_\ell \tilde{\mathbf{u}}_\ell^\top \mathbf{H}^\top \Sigma^{-1} \mathbf{H} \tilde{\omega}_0^{(j)} + \sum_{\ell=1}^r \tilde{\mathbf{u}}_\ell \tilde{\mathbf{w}}_\ell^\top \frac{1}{i + c_\ell} \sum_{k=0}^{i-1} \boldsymbol{\varepsilon}_k^{(j)},\end{aligned}$$

where $c_\ell = \frac{1}{\tilde{\delta}_{\ell,0}}$ as before and we have used Corollary 4.5 to get the second line. We follow a similar argument to that for the bound on $\|\tilde{\mathcal{P}}\tilde{\theta}_i^{(j)}\|$ in the proof of Theorem 4.7, using that $\text{trace}(\tilde{\mathbf{u}}_\ell \tilde{\mathbf{u}}_\ell^\top) = \tilde{\mathbf{u}}_\ell^\top (\mathbf{H}^\top \Sigma^{-1} \mathbf{H})^{\frac{1}{2}} (\mathbf{H}^\top \Sigma^{-1} \mathbf{H})^\dagger (\mathbf{H}^\top \Sigma^{-1} \mathbf{H})^{\frac{1}{2}} \tilde{\mathbf{u}}_\ell \leq \|(\mathbf{H}^\top \Sigma^{-1} \mathbf{H})^\dagger\|$ and $\tilde{\mathbf{w}}_\ell^\top \Sigma \tilde{\mathbf{w}}_\ell = 1$, to obtain

$$\mathbb{E}[\|\tilde{\mathbb{P}}\tilde{\omega}_i^{(j)}\|^2] \leq \mathbb{E}[\|\tilde{\mathbb{P}}\tilde{\omega}_i^{(j)}\|^2] \leq \|(\mathbf{H}^\top \Sigma^{-1} \mathbf{H})^\dagger\| \sum_{\ell=1}^r \frac{i}{(i + c_\ell)^2} \leq \|(\mathbf{H}^\top \Sigma^{-1} \mathbf{H})^\dagger\| \left(\frac{r}{i}\right),$$

which is $\mathcal{O}(i^{-1})$, as $i \rightarrow \infty$. This gives the conclusion of (a). \square

5 Numerical illustration

We construct an illustrative example with $n = 8$ observations of $d = 12$ states, with randomly generated $\mathbf{H}, \Sigma, \mathbf{y}$, and $\mathbf{v}_0^{(j)}$ such that all fundamental subspaces are non-trivial, as follows: $\Sigma \in \mathbb{R}^{n \times n}$ is a random full-rank symmetric positive definite matrix, and $\mathbf{H} \in \mathbb{R}^{n \times d}$ is constructed so that $\text{Ker}(\mathbf{H})$ and $\text{Ker}(\mathbf{H}^\top)$ are both non-trivial. The observations \mathbf{y} are generated by applying \mathbf{H} to a random vector in \mathbb{R}^d and adding noise drawn from the normal distribution with mean zero and covariance Σ . The ensemble is initialized with J random particles that typically have nonzero components in both $\text{Ran}(\mathbf{H}^\top)$ and $\text{Ker}(\mathbf{H})$, but crucially, do *not* contain $\text{Ran}(\mathbf{H}^\top)$ within their span. For stochastic EKI we provide results for both a small ensemble with $J = 5$ particles and a large ensemble with $J = 40$ particles. For deterministic EKI we report results only for the small $J = 5$ ensemble. Our code for this example is available at <https://github.com/elizqian/eki-fundamental-subspaces>.

Figure 3 plots the magnitude of the components of the observation space misfit and the state space residual of the EKI particles under both the deterministic and stochastic EKI dynamics. For both deterministic and stochastic EKI, the projectors are computed from the eigenvalue problems defined by the initial ensemble. Solid blue lines show the misfit/residual components projected by \mathcal{P}/\mathbb{P} onto observable and populated space: for deterministic EKI, and for stochastic EKI with a large ensemble, we observe convergence at the expected $1/\sqrt{i}$ rate in this space, but stochastic EKI with a small ensemble fails to converge, because with only $J = 5$ particles the true iterations eqs. (4.1) and (4.10) are far from their idealized counterparts eqs. (4.5) and (4.12). Dashed orange lines show the misfit/residual components projected by \mathcal{Q}/\mathbb{Q} onto observable and unpopulated space: because there are no particles in this space, this component remains constant for both deterministic and stochastic EKI regardless of the ensemble size. Finally, dotted gray lines show the misfit/residual components projected by \mathcal{N}/\mathbb{N} onto the unobservable space, which remain constant for deterministic EKI and approximately constant for stochastic EKI. Deviations in stochastic EKI behavior in the \mathcal{P}/\mathbb{P} and \mathcal{N}/\mathbb{N} subspaces from the theoretical results of Theorems 4.7 and 4.12 reflect deviations of the true iterations eqs. (4.1) and (4.10) from their idealized analogues eqs. (4.5) and (4.12).

6 Conclusions

The work presented here offers a new analysis of the behavior of both deterministic and stochastic versions of basic EKI for linear observation operators, interpreting EKI convergence properties in terms of “fundamental subspaces” analogous to Strang’s fundamental subspaces of linear algebra. Our analysis directly examines the discrete EKI iteration and defines six fundamental subspaces across both observation and state spaces that

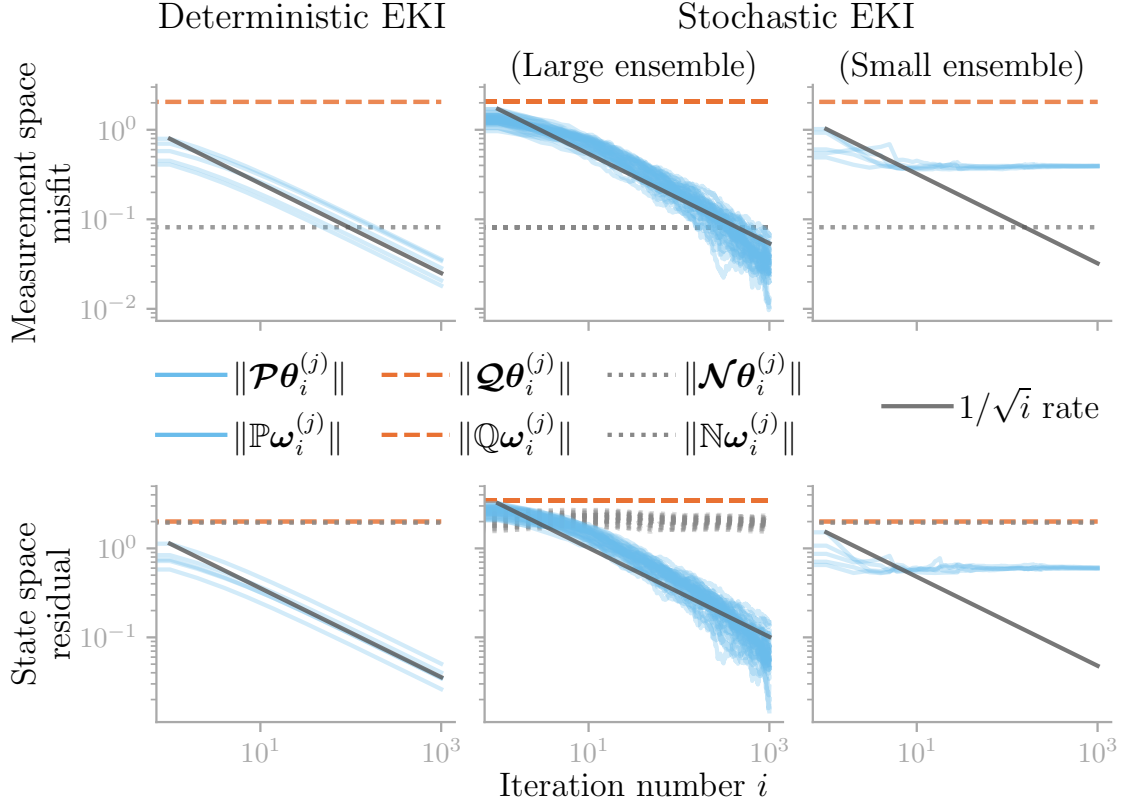


Figure 3: Evolution of particle misfit/residual components under deterministic and stochastic variants of EKI. Deterministic EKI and stochastic EKI small ensemble results use $J = 5$ particles; the large stochastic EKI ensemble uses $J = 40$ particles for a randomly generated problem with dimensions $n = 8$ and $d = 12$.

are distinguished in terms of convergence behaviour. This approach confirms convergence rates previously derived elsewhere for continuous-time limits and yields new results that describe EKI behavior in terms of these fundamental subspaces. Our analysis is the first to illuminate the relationship between EKI solutions and the standard minimum-norm weighted least squares solution: EKI particles converge to the standard solution only in the observable and populated fundamental subspace, while particle components in the unpopulated observable space and unobservable space remain at their initialized values.

We note that the fundamental subspaces of EKI that we describe are independent of the iteration index i , while convergence rates within these subspaces are governed by the magnitude of eigenvalues related to the invariant subspaces. Similar circumstances occur in classical iterative methods for solving linear systems (e.g., see the discussion of Richardson iteration in [7, Sect. 6.1.3]), suggesting directions for further EKI methodological development and analysis that exploit these connections. For example, EKI variants based on convergence acceleration for classical iterative methods may be pursued as an alternative to convergence acceleration based on covariance inflation. Future work will investigate these ideas further.

Acknowledgments

Work by EQ was supported in parts by the US Department of Energy Office of Science Energy Earthshot Initiative as part of the ‘Learning reduced models under extreme data conditions for design and rapid decision-making in complex systems’ project under award number DE-SC0024721, and by the Air Force Office of Scientific Research (AFOSR) award FA9550-24-1-0105 (Program Officer Dr. Fariba Fahroo). CB was supported in part by the National Science Foundation under DMS-2318880.

A Additional results concerning stochastic EKI

Proposition A.1. *For $i \geq 0$, $\mathbb{E}[\mathbf{H}\mathbf{\Gamma}_i\mathbf{H}^\top] \leq \mathbf{C}_i$, with respect to Löwner ordering.*

Proof. We proceed by induction. The statement is trivially true at $i = 0$ since $\mathbb{E}[\mathbf{H}\mathbf{\Gamma}_0\mathbf{H}^\top] = \mathbf{H}\mathbf{\Gamma}_0\mathbf{H}^\top = \mathbf{C}_0$. Now take the expectation of (4.3) over all stochastic perturbations and use the Law of Iterated Expectation to obtain

$$\begin{aligned}\mathbb{E}[\mathbf{H}\mathbf{\Gamma}_{i+1}\mathbf{H}^\top] &= \mathbb{E}\left[\mathbb{E}[\mathbf{H}\mathbf{\Gamma}_{i+1}\mathbf{H}^\top | \boldsymbol{\varepsilon}_{0:i-1}^{(1:J)}]\right] = \mathbb{E}[\boldsymbol{\Sigma} - \boldsymbol{\Sigma}(\mathbf{H}\mathbf{\Gamma}_i\mathbf{H}^\top + \boldsymbol{\Sigma})^{-1}\boldsymbol{\Sigma}] \\ &= \boldsymbol{\Sigma} - \boldsymbol{\Sigma}\mathbb{E}[(\mathbf{H}\mathbf{\Gamma}_i\mathbf{H}^\top + \boldsymbol{\Sigma})^{-1}]\boldsymbol{\Sigma} \leq \boldsymbol{\Sigma} - \boldsymbol{\Sigma}(\mathbb{E}[\mathbf{H}\mathbf{\Gamma}_i\mathbf{H}^\top] + \boldsymbol{\Sigma})^{-1}\boldsymbol{\Sigma},\end{aligned}\tag{A.1}$$

where the inequality comes from the convexity of the inverse within the family of positive definite matrices. The inductive hypothesis together with (A.1) implies that

$$\mathbb{E}[\mathbf{H}\mathbf{\Gamma}_{i+1}\mathbf{H}^\top] \leq \boldsymbol{\Sigma} - \boldsymbol{\Sigma}(\mathbf{C}_i + \boldsymbol{\Sigma})^{-1}\boldsymbol{\Sigma} = \mathbf{C}_{i+1},$$

where the inequality follows because the function $f(\mathbf{X}) = \boldsymbol{\Sigma} - \boldsymbol{\Sigma}(\mathbf{X} + \boldsymbol{\Sigma})^{-1}\boldsymbol{\Sigma}$ is non-decreasing with respect to \mathbf{X} in the Löwner ordering. \square

Proposition A.2. *$\|\tilde{\mathcal{P}}\tilde{\boldsymbol{\theta}}_i^{(j)}\| \rightarrow 0$ in probability at a rate that can be made arbitrarily close to $1/\sqrt{i}$. That is, $\lim_{i \rightarrow \infty} \text{Prob}\left(\|\tilde{\mathcal{P}}\tilde{\boldsymbol{\theta}}_i^{(j)}\| \geq \frac{\varepsilon}{i^p}\right) = 0$ for all $0 < p < \frac{1}{2}$ and all $\varepsilon > 0$. In the $i \rightarrow \infty$ limit, $\tilde{\mathcal{P}}\tilde{\boldsymbol{\theta}}_i^{(j)}$ converges to zero almost surely.*

Proof. Note first that for any $\varepsilon > 0$, the event $\|\tilde{\mathcal{P}}\tilde{\boldsymbol{\theta}}_i^{(j)}\| \geq \frac{\varepsilon}{i^p}$ is identical to the event $\|\tilde{\mathcal{P}}\tilde{\boldsymbol{\theta}}_i^{(j)}\|^2 \geq \frac{\varepsilon^2}{i^{2p}}$ and so by the Markov inequality and (4.9),

$$\text{Prob}\left(\|\tilde{\mathcal{P}}\tilde{\boldsymbol{\theta}}_i^{(j)}\| \geq \frac{\varepsilon}{i^p}\right) = \text{Prob}\left(\|\tilde{\mathcal{P}}\tilde{\boldsymbol{\theta}}_i^{(j)}\|^2 \geq \frac{\varepsilon^2}{i^{2p}}\right) \leq \frac{i^{2p}}{\varepsilon^2} \mathbb{E}\left[\|\tilde{\mathcal{P}}\tilde{\boldsymbol{\theta}}_i^{(j)}\|^2\right] \leq \|\boldsymbol{\Sigma}\| \left(\frac{r}{\varepsilon^2}\right) \cdot i^{2p-1}.$$

So, $\lim_{i \rightarrow \infty} \text{Prob}\left(\|\tilde{\mathcal{P}}\tilde{\boldsymbol{\theta}}_i^{(j)}\| \geq \frac{\varepsilon}{i^p}\right) = 0$ for all $0 < p < \frac{1}{2}$, establishing the first assertion. For the second assertion, rewrite $\tilde{\mathcal{P}}\tilde{\boldsymbol{\theta}}_i^{(j)}$ as

$$\tilde{\mathcal{P}}\tilde{\boldsymbol{\theta}}_i^{(j)} = \frac{1}{i} \sum_{\ell=1}^r \frac{i c_\ell}{i + c_\ell} \boldsymbol{\Sigma} \tilde{\mathbf{w}}_\ell \tilde{\mathbf{w}}_\ell^\top \left(\tilde{\mathcal{P}}\tilde{\boldsymbol{\theta}}_0^{(j)}\right) + \sum_{\ell=1}^r \frac{i}{i + c_\ell} \boldsymbol{\Sigma} \tilde{\mathbf{w}}_\ell \tilde{\mathbf{w}}_\ell^\top \left(\frac{1}{i} \sum_{k=0}^{i-1} \boldsymbol{\varepsilon}_k^{(j)}\right).$$

The first term is non-stochastic and converges to $\mathbf{0}$ as $i \rightarrow \infty$. The second term involves the average of a sequence of *i.i.d.* random vectors: $\mathbf{m}_i^{(j)} = \frac{1}{i} \sum_{k=0}^{i-1} \boldsymbol{\varepsilon}_k^{(j)}$, which by *the strong law of large numbers* converges almost surely to $\mathbf{0}$, the common mean of $\boldsymbol{\varepsilon}_k^{(j)}$: $\mathbf{m}_i^{(j)} \xrightarrow{a.s.} \mathbf{0}$. Hence, $\tilde{\mathcal{P}}\tilde{\boldsymbol{\theta}}_i^{(j)}$ also converges almost surely to $\mathbf{0}$ as $i \rightarrow \infty$. \square

Proposition A.3. $\text{Prob}(\mathbf{H}\boldsymbol{\Gamma}_i\mathbf{H}^\top \leq \varepsilon \boldsymbol{\Sigma}) \geq 1 - \frac{n}{\varepsilon} \frac{1}{i}$ for $\varepsilon > 0$. As a consequence, $\lim_{i \rightarrow \infty} \text{Prob}\left(\mathbf{H}\boldsymbol{\Gamma}_i\mathbf{H}^\top \leq \frac{1}{i^p} \boldsymbol{\Sigma}\right) = 1$ for all $0 < p < 1$, so $\mathbf{H}\boldsymbol{\Gamma}_i\mathbf{H}^\top \rightarrow \mathbf{0}$ in probability at a rate that can be made arbitrarily close to $\frac{1}{i}$. Likewise, $\boldsymbol{\mathcal{M}}_i \rightarrow \mathbf{I}$ in probability as $i \rightarrow \infty$.

Proof. A matrix version of the Markov inequality (see e.g., [1, Theorem 12]) can be stated as: if \mathbf{X} is a random symmetric matrix with finite expectation that is positive semidefinite almost surely (meaning $\text{Prob}(\mathbf{X} \geq \mathbf{0}) = 1$), then for any $\varepsilon > 0$, $\text{Prob}(\mathbf{X} \leq \varepsilon \mathbf{I}) \geq 1 - \frac{1}{\varepsilon} \text{trace}(\mathbb{E}[\mathbf{X}])$. Choosing $\mathbf{X} = \boldsymbol{\Sigma}^{-\frac{1}{2}} \mathbf{H}\boldsymbol{\Gamma}_i\mathbf{H}^\top \boldsymbol{\Sigma}^{-\frac{1}{2}}$, we have $\mathbf{X} \leq \varepsilon \mathbf{I}$ if and only if $\mathbf{H}\boldsymbol{\Gamma}_i\mathbf{H}^\top \leq \varepsilon \boldsymbol{\Sigma}$, so $\text{Prob}(\mathbf{H}\boldsymbol{\Gamma}_i\mathbf{H}^\top \leq \varepsilon \boldsymbol{\Sigma}) = \text{Prob}(\mathbf{X} \leq \varepsilon \mathbf{I})$. Combining Proposition A.1 with equation (4.6) and Corollary 4.5 gives

$$\text{trace}(\mathbb{E}[\boldsymbol{\Sigma}^{-\frac{1}{2}} \mathbf{H}\boldsymbol{\Gamma}_i\mathbf{H}^\top \boldsymbol{\Sigma}^{-\frac{1}{2}}]) \leq \text{trace}(\boldsymbol{\Sigma}^{-\frac{1}{2}} \mathbf{C}_i \boldsymbol{\Sigma}^{-\frac{1}{2}}) = \sum_{\ell=1}^n \tilde{\delta}_{\ell,i} = \sum_{\ell=1}^n \frac{1}{\tilde{\delta}_{\ell,0} + i} \leq \frac{n}{i},$$

which leads to the first bound. The second assertion follows from choosing $\varepsilon = \frac{1}{i^p}$ and taking the limit $i \rightarrow \infty$. This implies, in particular, convergence of $\mathbf{H}\boldsymbol{\Gamma}_i\mathbf{H}^\top \rightarrow \mathbf{0}$ in probability at a rate of $\frac{1}{i^p}$. Observe that $\boldsymbol{\mathcal{M}}_i = \boldsymbol{\Sigma}(\mathbf{H}\boldsymbol{\Gamma}_i\mathbf{H}^\top + \boldsymbol{\Sigma})^{-1} = \mathbf{I} - \mathbf{H}\boldsymbol{\Gamma}_i\mathbf{H}^\top(\mathbf{H}\boldsymbol{\Gamma}_i\mathbf{H}^\top + \boldsymbol{\Sigma})^{-1}$ and so, $\boldsymbol{\mathcal{M}}_i$ is a continuous function of $\mathbf{H}\boldsymbol{\Gamma}_i\mathbf{H}^\top$. Since $\mathbf{H}\boldsymbol{\Gamma}_i\mathbf{H}^\top \rightarrow \mathbf{0}$ in probability, we have that $\boldsymbol{\mathcal{M}}_i \rightarrow \mathbf{I}$ in probability as $i \rightarrow \infty$ as well. \square

References

- [1] R. AHLWEDE AND A. WINTER, *Strong converse for identification via quantum channels*, IEEE Transactions on Information Theory, 48 (2002), pp. 569–579.
- [2] D. J. ALBERS, P.-A. BLANCQUART, M. E. LEVINE, E. ESMAEILZADEH SEYLABI, AND A. STUART, *Ensemble Kalman methods with constraints*, Inverse Problems, 35 (2019), p. 095007, <https://doi.org/10.1088/1361-6420/ab1c09>.
- [3] D. ARMBRUSTER, M. HERTY, AND G. VISCONTI, *A Stabilization of a Continuous Limit of the Ensemble Kalman Inversion*, SIAM Journal on Numerical Analysis, 60 (2022), pp. 1494–1515, <https://doi.org/10.1137/21M1414000>.
- [4] E. E. BAS, E. SEYLABI, A. YONG, H. TEHRANI, AND D. ASIMAKI, *P- and S-wave velocity estimation by ensemble Kalman inversion of dispersion data for strong motion stations in California*, Geophysical Journal International, 231 (2022), pp. 536–551, <https://doi.org/10.1093/gji/ggac201>.
- [5] K. BERGEMANN AND S. REICH, *A localization technique for ensemble Kalman filters*, Jan. 2010, <https://doi.org/10.48550/arXiv.0909.1678>, <https://arxiv.org/abs/0909.1678>.
- [6] K. BERGEMANN AND S. REICH, *A mollified Ensemble Kalman filter*, Quarterly Journal of the Royal Meteorological Society, 136 (2010), pp. 1636–1643, <https://doi.org/10.1002/qj.672>, <https://arxiv.org/abs/1002.3091>.
- [7] Å. BJÖRCK, *Numerical methods for least squares problems*, SIAM, 2024.
- [8] D. BLÖMKER, C. SCHILLINGS, AND P. WACKER, *A strongly convergent numerical scheme from ensemble Kalman inversion*, SIAM Journal on Numerical Analysis, 56 (2018), pp. 2537–2562.
- [9] D. BLÖMKER, C. SCHILLINGS, P. WACKER, AND S. WEISSMANN, *Well posedness and convergence analysis of the ensemble Kalman inversion*, Inverse Problems, 35 (2019), p. 085007.

- [10] D. BLÖMKER, C. SCHILLINGS, P. WACKER, AND S. WEISSMANN, *Continuous time limit of the stochastic ensemble Kalman inversion: Strong convergence analysis*, SIAM Journal on Numerical Analysis, 60 (2022), pp. 3181–3215.
- [11] M. BOCQUET, J. BRAJARD, A. CARRASSI, AND L. BERTINO, *Bayesian inference of chaotic dynamics by merging data assimilation, machine learning and expectation-maximization*, Foundations of Data Science, 2 (2020), pp. 55–80, <https://doi.org/10.3934/fods.2020004>, <https://arxiv.org/abs/2001.06270>.
- [12] L. BUNGERT AND P. WACKER, *Complete deterministic dynamics and spectral decomposition of the linear ensemble Kalman inversion*, SIAM/ASA Journal on Uncertainty Quantification, 11 (2023), pp. 320–357.
- [13] E. CALVELLO, S. REICH, AND A. M. STUART, *Ensemble Kalman methods: A mean field perspective*, arXiv preprint arXiv:2209.11371, (2022).
- [14] J. A. CARRILLO, C. TOTZECK, AND U. VAES, *Consensus-Based Optimization and Ensemble Kalman Inversion for Global Optimization Problems with Constraints*, vol. 40, WORLD SCIENTIFIC, 2023, pp. 195–230, https://doi.org/10.1142/9789811266140_0004.
- [15] N. CHADA AND X. TONG, *Convergence acceleration of ensemble Kalman inversion in nonlinear settings*, Mathematics of Computation, 91 (2022), pp. 1247–1280.
- [16] N. K. CHADA, *Analysis of Hierarchical Ensemble Kalman Inversion*, 2018, <https://arxiv.org/abs/1801.00847>.
- [17] N. K. CHADA, Y. CHEN, AND D. SANZ-ALONSO, *Iterative ensemble Kalman methods: A unified perspective with some new variants*, Foundations of Data Science, 3 (2021), p. 331, <https://doi.org/10.3934/fods.2021011>.
- [18] N. K. CHADA, C. SCHILLINGS, AND S. WEISSMANN, *On the Incorporation of Box-Constraints for Ensemble Kalman Inversion*, 2019, <https://arxiv.org/abs/1908.00696>.
- [19] N. K. CHADA, A. M. STUART, AND X. T. TONG, *Tikhonov regularization within ensemble kalman inversion*, SIAM Journal on Numerical Analysis, 58 (2020), pp. 1263–1294, <https://doi.org/10.1137/19M1242331>.
- [20] Y. CHEN AND D. S. OLIVER, *Ensemble Randomized Maximum Likelihood Method as an Iterative Ensemble Smoother*, Mathematical Geosciences, 44 (2012), pp. 1–26, <https://doi.org/10.1007/s11004-011-9376-z>.
- [21] N. CHOPIN, O. PAPASPILIOPOULOS, ET AL., *An introduction to sequential Monte Carlo*, vol. 4, Springer, 2020.
- [22] J. CHUNG, J. G. NAGY, AND I. SECHOPOULOS, *Numerical algorithms for polyenergetic digital breast tomosynthesis reconstruction*, SIAM Journal on Imaging Sciences, 3 (2010), pp. 133–152.
- [23] E. CLEARY, A. GARBUNO-INIGO, S. LAN, T. SCHNEIDER, AND A. M. STUART, *Calibrate, emulate, sample*, Journal of Computational Physics, 424 (2021), p. 109716, <https://doi.org/10.1016/j.jcp.2020.109716>.
- [24] F. DAUM, J. HUANG, AND A. NOUSHIN, *Exact particle flow for nonlinear filters*, in Signal processing, sensor fusion, and target recognition XIX, vol. 7697, SPIE, 2010, pp. 92–110.
- [25] P. DEL MORAL, A. DOUCET, AND A. JASRA, *Sequential Monte Carlo Samplers*, Journal of the Royal Statistical Society Series B: Statistical Methodology, 68 (2006), pp. 411–436, <https://doi.org/10.1111/j.1467-9868.2006.00553.x>.
- [26] Z. DING AND Q. LI, *Ensemble Kalman inversion: mean-field limit and convergence analysis*, Statistics and Computing, 31 (2021), pp. 1–21.

- [27] O. R. A. DUNBAR, A. GARBUNO-INIGO, T. SCHNEIDER, AND A. M. STUART, *Calibration and Uncertainty Quantification of Convective Parameters in an Idealized GCM*, Journal of Advances in Modeling Earth Systems, 13 (2021), p. e2020MS002454, <https://doi.org/10.1029/2020MS002454>.
- [28] A. A. EMERICK AND A. C. REYNOLDS, *Ensemble smoother with multiple data assimilation*, Computers & Geosciences, 55 (2013), pp. 3–15, <https://doi.org/10.1016/j.cageo.2012.03.011>.
- [29] A. A. EMERICK AND A. C. REYNOLDS, *Investigation of the sampling performance of ensemble-based methods with a simple reservoir model*, Computational Geosciences, 17 (2013), pp. 325–350, <https://doi.org/10.1007/s10596-012-9333-z>.
- [30] C. L. EPSTEIN, *Introduction to the mathematics of medical imaging*, SIAM, 2007.
- [31] G. EVENSEN, *Analysis of iterative ensemble smoothers for solving inverse problems*, Computational Geosciences, 22 (2018), pp. 885–908, <https://doi.org/10.1007/s10596-018-9731-y>.
- [32] G. A. GOTTWALD AND S. REICH, *Supervised learning from noisy observations: Combining machine-learning techniques with data assimilation*, Physica D: Nonlinear Phenomena, 423 (2021), p. 132911, <https://doi.org/10.1016/j.physd.2021.132911>, <https://arxiv.org/abs/2007.07383>.
- [33] Y. GU AND D. S. OLIVER, *An Iterative Ensemble Kalman Filter for Multiphase Fluid Flow Data Assimilation*, SPE Journal, 12 (2007), pp. 438–446, <https://doi.org/10.2118/108438-PA>.
- [34] P. A. GUTH, C. SCHILLINGS, AND S. WEISSMANN, *14 Ensemble Kalman filter for neural network-based one-shot inversion*, in 14 Ensemble Kalman Filter for Neural Network-Based One-Shot Inversion, De Gruyter, 2022, pp. 393–418, <https://doi.org/10.1515/9783110695984-014>.
- [35] M. HANU, J. LATZ, AND C. SCHILLINGS, *Subsampling in ensemble Kalman inversion*, Inverse Problems, 39 (2023), p. 094002, <https://doi.org/10.1088/1361-6420/ace64b>.
- [36] M. HANU AND S. WEISSMANN, *On the ensemble Kalman inversion under inequality constraints*, Inverse Problems, (2024), <https://doi.org/10.1088/1361-6420/ad6a33>.
- [37] M. HERTY AND G. VISCONTI, *Kinetic Methods for Inverse Problems*, 2019, <https://doi.org/10.48550/arXiv.1811.09387>, <https://arxiv.org/abs/1811.09387>.
- [38] R. A. HORN AND C. R. JOHNSON, *Matrix analysis*, Cambridge university press, 2012.
- [39] D. Z. HUANG, J. HUANG, S. REICH, AND A. M. STUART, *Efficient derivative-free Bayesian inference for large-scale inverse problems*, Inverse Problems, 38 (2022), p. 125006, <https://doi.org/10.1088/1361-6420/ac99fa>.
- [40] M. IGLESIAS, D. M. MCGRATH, M. V. TRETYAKOV, AND S. T. FRANCIS, *Ensemble Kalman inversion for magnetic resonance elastography*, Physics in Medicine & Biology, 67 (2022), p. 235003, <https://doi.org/10.1088/1361-6560/ac9fa1>.
- [41] M. A. IGLESIAS, K. J. H. LAW, AND A. M. STUART, *Ensemble Kalman methods for inverse problems*, Inverse Problems, 29 (2013), p. 045001.
- [42] M. A. IGLESIAS, K. LIN, AND A. M. STUART, *Well-posed bayesian geometric inverse problems arising in subsurface flow*, Inverse Problems, 30 (2014), p. 114001.
- [43] N. B. KOVACHKI AND A. M. STUART, *Ensemble Kalman inversion: A derivative-free technique for machine learning tasks*, Inverse Problems, 35 (2019), p. 095005, <https://doi.org/10.1088/1361-6420/ab1c3a>.
- [44] G. LI AND A. C. REYNOLDS, *Iterative Ensemble Kalman Filters for Data Assimilation*, SPE Journal, 14 (2009), pp. 496–505, <https://doi.org/10.2118/109808-PA>.
- [45] S. LIU, S. REICH, AND X. T. TONG, *Dropout ensemble Kalman inversion for high dimensional inverse problems*, arXiv preprint arXiv:2308.16784, (2023).

- [46] I. LOPEZ-GOMEZ, C. CHRISTOPOULOS, H. L. LANGE LAND ERVIK, O. R. A. DUNBAR, Y. COHEN, AND T. SCHNEIDER, *Training Physics-Based Machine-Learning Parameterizations With Gradient-Free Ensemble Kalman Methods*, Journal of Advances in Modeling Earth Systems, 14 (2022), p. e2022MS003105, <https://doi.org/10.1029/2022MS003105>.
- [47] S. MAJUMDER, R. M. CASTELAO, AND C. M. AMOS, *Freshwater variability and transport in the labrador sea from in situ and satellite observations*, Journal of Geophysical Research: Oceans, 126 (2021), p. e2020JC016751.
- [48] H. NGUYEN, N. CRESSIE, AND A. BRAVERMAN, *Spatial statistical data fusion for remote sensing applications*, Journal of the American Statistical Association, 107 (2012), pp. 1004–1018.
- [49] H. J. PALANTHANDALAM-MADAPUSI, A. GIRARD, AND D. S. BERNSTEIN, *Wind-field reconstruction using flight data*, in 2008 American control conference, IEEE, 2008, pp. 1863–1868.
- [50] G. PANTELEEV, M. YAREMCHUK, AND W. E. ROGERS, *Adjoint-free variational data assimilation into a regional wave model*, Journal of Atmospheric and Oceanic Technology, 32 (2015), pp. 1386–1399.
- [51] F. PARZER AND O. SCHERZER, *On convergence rates of adaptive ensemble Kalman inversion for linear ill-posed problems*, Numerische Mathematik, 152 (2022), pp. 371–409, <https://doi.org/10.1007/s00211-022-01314-y>.
- [52] A. PENSONEAULT, W. F. KRAJEWSKI, N. VELÁSQUEZ, X. ZHU, AND R. MANTILLA, *Ensemble Kalman Inversion for upstream parameter estimation and indirect streamflow correction: A simulation study*, Advances in Water Resources, 181 (2023), p. 104545, <https://doi.org/10.1016/j.advwatres.2023.104545>.
- [53] J. PIDSTRIGACH AND S. REICH, *Affine-Invariant Ensemble Transform Methods for Logistic Regression*, Foundations of Computational Mathematics, 23 (2023), pp. 675–708, <https://doi.org/10.1007/s10208-022-09550-2>.
- [54] M. PULIDO, P. TANDEO, M. BOCQUET, A. CARRASSI, AND M. LUCINI, *Stochastic parameterization identification using ensemble Kalman filtering combined with maximum likelihood methods*, Tellus A: Dynamic Meteorology and Oceanography, 70 (2018), pp. 1–17, <https://doi.org/10.1080/16000870.2018.1442099>.
- [55] S. REICH AND C. COTTER, *Probabilistic forecasting and Bayesian data assimilation*, Cambridge University Press, 2015.
- [56] P. SAKOV, D. S. OLIVER, AND L. BERTINO, *An iterative EnKF for strongly nonlinear systems*, Monthly Weather Review, 140 (2012), pp. 1988–2004.
- [57] O. SCHERZER, *Mathematical models for registration and applications to medical imaging*, vol. 10, Springer Science & Business Media, 2006.
- [58] C. SCHILLINGS AND A. M. STUART, *Analysis of the ensemble Kalman filter for inverse problems*, SIAM Journal on Numerical Analysis, 55 (2017), pp. 1264–1290.
- [59] C. SCHILLINGS AND A. M. STUART, *Convergence analysis of ensemble Kalman inversion: the linear, noisy case*, Applicable Analysis, 97 (2018), pp. 107–123.
- [60] T. SCHNEIDER, S. LAN, A. STUART, AND J. TEIXEIRA, *Earth System Modeling 2.0: A Blueprint for Models That Learn From Observations and Targeted High-Resolution Simulations*, Geophysical Research Letters, 44 (2017), pp. 12,396–12,417, <https://doi.org/10.1002/2017GL076101>.
- [61] T. SCHNEIDER, A. M. STUART, AND J.-L. WU, *Learning stochastic closures using ensemble Kalman inversion*, Transactions of Mathematics and Its Applications, 5 (2021), p. tnab003, <https://doi.org/10.1093/imatrm/tnab003>.

- [62] T. SCHNEIDER, A. M. STUART, AND J.-L. WU, *Ensemble Kalman inversion for sparse learning of dynamical systems from time-averaged data*, Journal of Computational Physics, 470 (2022), p. 111559, <https://doi.org/10.1016/j.jcp.2022.111559>.
- [63] G. STRANG, *The fundamental theorem of linear algebra*, The American Mathematical Monthly, 100 (1993), pp. 848–855.
- [64] X. TONG AND M. MORZFELD, *Localized ensemble Kalman inversion*, Inverse Problems, 39 (2023), p. 064002.
- [65] C.-H. M. TSO, M. IGLESIAS, AND A. BINLEY, *Ensemble Kalman inversion of induced polarization data*, Geophysical Journal International, 236 (2024), pp. 1877–1900, <https://doi.org/10.1093/gji/ggae012>.
- [66] S. TWOMEY, *Introduction to the mathematics of inversion in remote sensing and indirect measurements*, Elsevier, 2013.
- [67] F. WAGNER, I. PAPAIOANNOU, AND E. ULLMANN, *The Ensemble Kalman Filter for Rare Event Estimation*, SIAM/ASA Journal on Uncertainty Quantification, 10 (2022), pp. 317–349, <https://doi.org/10.1137/21M1404119>.
- [68] S. WEISSMANN, *Gradient flow structure and convergence analysis of the ensemble Kalman inversion for nonlinear forward models*, Inverse Problems, 38 (2022), p. 105011.
- [69] S. WEISSMANN, N. K. CHADA, C. SCHILLINGS, AND X. T. TONG, *Adaptive Tikhonov strategies for stochastic ensemble Kalman inversion*, Inverse Problems, 38 (2022), p. 045009, <https://doi.org/10.1088/1361-6420/ac5729>.
- [70] S. WEISSMANN, N. K. CHADA, AND X. T. TONG, *The Ensemble Kalman Filter for Dynamic Inverse Problems*, 2024, <https://arxiv.org/abs/2401.11948>.
- [71] S. WEISSMANN, A. WILSON, AND J. ZECH, *Multilevel optimization for inverse problems*, in Conference on Learning Theory, PMLR, 2022, pp. 5489–5524.
- [72] X.-L. ZHANG, L. ZHANG, AND G. HE, *Parallel ensemble Kalman method with total variation regularization for large-scale field inversion*, Journal of Computational Physics, 509 (2024), p. 113059, <https://doi.org/10.1016/j.jcp.2024.113059>.